
ALGORITHMS FOR MINIMAL PICARD-FUCHS OPERATORS OF FEYNMAN INTEGRALS

by

Pierre Lairez & Pierre Vanhove

Abstract. — In even space-time dimensions the multi-loop Feynman integrals are integrals of rational function in projective space. By using an algorithm that extends the Griffiths–Dwork reduction for the case of projective hypersurfaces with singularities, we derive Fuchsian linear differential equations, the Picard–Fuchs equations, with respect to kinematic parameters for a large class of massive multi-loop Feynman integrals. With this approach we obtain the differential operator for Feynman integrals to high multiplicities and high loop orders. Using recent factorisation algorithms we give the minimal order differential operator in most of the cases studied in this paper. Amongst our results are that the order of Picard–Fuchs operator for the generic massive two-point $n - 1$ -loop sunset integral in two-dimensions is $2^n - \binom{n+1}{\lfloor \frac{n+1}{2} \rfloor}$ supporting the conjecture that the sunset Feynman integrals are relative periods of Calabi–Yau of dimensions $n - 2$. We have checked this explicitly till six loops. As well, we obtain a particular Picard–Fuchs operator of order 11 for the massive five-point tardigrade non-planar two-loop integral in four dimensions for generic mass and kinematic configurations, suggesting that it arises from $K3$ surface with Picard number 11. We determine as well Picard–Fuchs operators of two-loop graphs with various multiplicities in four dimensions, finding Fuchsian differential operators with either Liouvillian or elliptic solutions.

Contents

1. Introduction.....	3
2. Feynman integrals.....	7
2.1. Definitions and notations.....	7
2.2. Feynman integral as relative period integrals.....	9
2.3. Feynman integral differential equations.....	10
2.4. Relations between various integrals.....	11
3. Picard–Fuchs equations for Feynman integrals	12
3.1. The Griffiths–Dwork reduction.....	14
3.2. Picard–Fuchs equations in the smooth case.....	15
3.3. An extension of the Griffiths–Dwork reduction...	16
4. The multiloop sunset graphs.....	18
4.1. One-loop sunset.....	21
4.2. Two-loop sunset.....	22
4.3. Three-loop sunset.....	23
4.3.1. Mass specialisation.....	26
4.4. The four-loop sunset.....	26
4.4.1. Mass specialisation.....	28
4.5. The five-loop sunset.....	29
4.6. The six-loop sunset.....	30
5. The multi-scoop ice-cream graphs.....	31
5.1. The zero-scoop ice-cream (triangle) graph.....	32
5.2. The one-scoop ice-cream graph.....	34
5.3. The two-scoop ice-cream graph.....	36
6. Some two-loop graphs differential operator.....	37
6.1. The kite graph.....	38
6.1.1. Triviality of the kite integral in two dimensions	38
6.1.2. The kite integral in four dimensions.....	41
6.2. The tardigrade.....	42
6.2.1. The three points case.....	43
6.2.2. The five points case.....	44
6.3. The double-box graphs.....	45
6.4. The pentabox graphs.....	47
7. Conclusion.....	50
Acknowledgments.....	51
References.....	52

1. Introduction

Feynman integrals enter the evaluation of many physical observable quantities in particle physics, gravitational physics, statistical physics, and solid-state physics. They are multi-valued functions, with non-trivial monodromies. They present branch cuts (associated with particle production) and their analytic or numerical evaluations are challenging. The identification of the kind of special functions needed to evaluate the Feynman integrals is difficult question under study from the early days of Quantum field theory [1, 2] and is still an active field of research e.g. [3, 4, 5].

Broadhurst and Kreimer [6, 7] remarked that the definition of the Feynman integrals resembles the definition of period integrals given by Kontsevich and Zagier in [8]. Bloch, Esnault, and Kreimer showed [9] that the Feynman integral is a relative period integral of the mixed Hodge structure determined by the graph polynomials defining the Feynman integrals. There are increasing evidence that some Feynman integrals are relative periods integrals of (singular) Calabi–Yau geometries [10, 11, 12, 13, 14, 15, 16, 17, 18, 19, 20, 21].

One aim of this work is to sharpen this correspondence by deriving Picard–Fuchs differential operators associated to the Feynman integrals by studying the case where a Feynman integral $I_\Gamma(t) = \int_{\Delta_n} \Omega_\Gamma(t)$ is given by the integral over the positive orthant Δ_n , defined in (2.2), of rational differential form in projective space

$$\Omega_\Gamma(t) = \frac{\mathcal{U}(\underline{x})^{n-(L+1)r}}{(\mathcal{F}_0(\underline{x}) + t\mathcal{F}_1(\underline{x}))^{n-Lr}} \Omega_0^{(n)} \quad (1.1)$$

with n , L and r positive integers with $n - Lr > 0$, and $\underline{x} := [x_1 : \cdots : x_n] \in \mathbb{P}^{n-1}$, $\Omega_0^{(n)}$ is the canonical differential form on \mathbb{P}^{n-1} , given in (2.4). The homogeneous polynomial $\mathcal{U}(\underline{x})$ has degree L and the homogeneous polynomials $\mathcal{F}_0(\underline{x})$ and $\mathcal{F}_1(\underline{x})$ have degree $L + 1$ so that the integrand is

a well-defined rational differential form. We will restrict to the case of converging integrals.

Our approach uses an implementation of the Griffiths–Dwork reduction algorithm adapted to the case of period of rational integrals with non-isolated singularities. We construct a Fuchsian differential operator in the variable t annihilating the integrand

$$\left(\mathcal{L}_t - \mathcal{C}(t, \partial_t; \partial_{\underline{x}}, \underline{x})\right) \frac{\mathcal{U}(\underline{x})^{n-(L+1)r}}{(\mathcal{F}_0(\underline{x}) + t\mathcal{F}_1(\underline{x}))^{n-Lr}} = 0. \quad (1.2)$$

This annihilator is composed of a Picard–Fuchs differential operator acting only on the parameter t

$$\mathcal{L}_t = \sum_{r=0}^{o_n} p_r(t) \left(\frac{d}{dt}\right)^r \quad (1.3)$$

and a certificate part

$$\mathcal{C}(t, \partial_t; \partial_{\underline{x}}, \underline{x}) = \sum_{i=1}^n \frac{\partial}{\partial x_i} Q_i(t, \partial_t; \partial_{\underline{x}}, \underline{x}) \quad (1.4)$$

with

$$Q_i(t, \partial_t; \partial_{\underline{x}}, \underline{x}) = \sum_{0 \leq a \leq a'_i} \sum_{\substack{0 \leq b_j \leq \sigma_j \\ 1 \leq j \neq n}} q_{a, b_1, \dots, b_r}^{(i)}(t; \underline{x}) \left(\frac{\partial}{\partial t}\right)^a \prod_{j=1}^n \left(\frac{\partial}{\partial x_j}\right)^{b_j}. \quad (1.5)$$

which are differential operators acting on the parameter t and the integration variables \underline{x} . From the identity (1.2) we deduce that the Feynman integral (1.1) satisfies the inhomogeneous differential equation

$$\mathcal{L}_t I_\Gamma(t) = \mathcal{S}(t). \quad (1.6)$$

The inhomogeneous term $\mathcal{S}(t)$ is a sum of the n contributions evaluated on the boundary components arising from the evaluation of the action of certificate on the integrand on the boundary of positive orthant. Each boundary component is a rational differential form for Feynman integral in \mathbb{P}^{n-2} with the same degree of polynomials (see [22]). For fixed values of

degree of homogeneity L and r , we are naturally led to study the rational periods integrals (1.1), with increasing values of n .

This work has two main aims. (1) The first one is to provide a convenient tool for exploring the relation between Feynman integrals and periods integrals. From the knowledge of the Picard–Fuchs operators \mathcal{L}_t we get an information (an upper bound) on the number of independent periods associated with the differential form (1.1). We check if the Picard–Fuchs operator is factorisable and when possible using the factorisation algorithm implemented in [23]. The irreducibility of the the Picard–Fuchs operator implies that the operator is minimal, but there are factorisable operator that are minimal as we will see in the case of the kite case in section 6.1. The analytic form of the Picard–Fuchs operators and their singularities provide an important hint about the algebraic geometry for which the Feynman integral is a relative period integral. We will find Picard–Fuchs operators suggestive of rational surfaces, elliptic curves, $K3$ surfaces, Calabi–Yau n -folds. By working with increasing values of n we determine if new types of periods arise from the homogeneous differential operator. (2) The second aim is to provide an efficient tools for deriving the differential equation for Feynman integrals numerically. The present algorithms give a way to analysis relatively high loop (we will study cases up to $L = 6$ loops order) and high multiplicities (we will study cases with up to seven external states) integrals.

The application of these techniques to Feynman integrals is described in [24]. But the implementation of the Griffiths–Dwork reduction algorithm is complicated by the presence of non-isolated singularities. For the case of the two-loop sunset integral one can apply the standard Griffiths–Dwork reduction algorithm for deriving the Picard–Fuchs operator (see 2.3.2 of [25]). But unlike the two-loop sunset integral, Feynman integrals have generically non-isolated singularities preventing a direct use of the Griffiths–Dwork reduction. We will use an extended version of the Griffiths–Dwork formalism adapted to the case with non-isolated

singularities that implement the pole reduction in the integrand using Syzygies [26].⁽¹⁾

In this work we will first recall the relation between the Feynman integrals and relative period integrals in section 2. In section 3 we describe the algorithm we will be using for deriving the Picard–Fuchs operators. In section 4 we derive the Picard–Fuchs operators for the sunset family of integral up to six-loop order with generic mass configurations. We show the factorisation of the Picard–Fuchs operator when specialising the mass configurations. In section 5 we consider the multi-scoop ice-cream graphs. We show how splitting an edge of the sunset graph affects the differential operator. In section 6 we give the differential operator for various two-loop integrals. We show the triviality of the kite integral in two dimensions. In four dimensions, we will obtain that the massive kite and massive double-box integral differential operator is order 2 compatible with an elliptic curve, and that the massive tardigrade differential operator is suggestive of a $K3$ surface with Picard number 11 for generic mass and kinematic configurations. We conclude with section 7.

We have collected various numerical results and expressions that are too long for being reported in this text on the following online pages

- The **identity** in eq. (3.5)
- The differential operators for the sunset graph at **2 loops**, **3 loops**, **4 loops**, **5 loops** analysed in section 4.
- The differential operators for the multiloop ice-cream graph at **1 loop**, **2 loops**, **3 loops** analysed in section 5
- The differential operators for the **kite graph** of section 6.1
- The differential operators for the **tardigrade graph** of section 6.2.
- The differential operators for the **double-box graph** of section 6.3
- The differential operators for the **pentabox graph** of section 6.4

⁽¹⁾A Magma implementation is available at github.com/lairez/periods.

2. Feynman integrals

In this section we review the connection between Feynman integrals and relative period integrals.

2.1. Definitions and notations. — The parametric representation of a Feynman integral associated to Feynman graph Γ , with n edges and L (homology) loops, is given by projective integral in $\mathbb{P}^{n-1}(\mathbb{R})$ in the variables (x_1, \dots, x_n) (see [9, 22, 27])

$$I_\Gamma(\underline{s}, \underline{m}^2; \underline{\nu}, D) = \int_{\Delta_n} \Omega_n(\underline{s}, \underline{m}^2; \underline{\nu}, D; \underline{x}), \quad (2.1)$$

where

- The domain of integral is the simplex defined by the positive quadrant

$$\Delta_n := \{[x_1, \dots, x_n] \in \mathbb{P}^{n-1} \mid x_i \in \mathbb{R}, x_i \geq 0\}. \quad (2.2)$$

- The differential form

$$\Omega_n(\underline{s}, \underline{m}^2; \underline{\nu}, D; \underline{x}) := \left(\frac{\mathcal{U}(\underline{x})}{\mathcal{U}(\underline{x})\mathcal{L}(\underline{m}^2, \underline{x}) - \mathcal{V}(\underline{s}, \underline{x})} \right)^\omega \frac{\prod_{i=1}^n x_i^{\nu_i-1} \Omega_0^{(n)}}{\mathcal{U}(\underline{x})^{\frac{D}{2}}} \quad (2.3)$$

and $\Omega_0^{(n)}$ is the natural differential $n-1$ -form on the real projective space \mathbb{P}^{n-1}

$$\Omega_0^{(n)} := \sum_{j=1}^n (-1)^{j-1} x_j dx_1 \wedge \cdots \wedge \widehat{dx_j} \wedge \cdots \wedge dx_n, \quad (2.4)$$

where $\widehat{dx_j}$ means that dx_j is omitted in this sum.

- The power

$$\omega = \sum_{i=1}^n \nu_i - \frac{LD}{2}, \quad (2.5)$$

with L a positive integer. The powers $(\nu_1, \dots, \nu_n) \in \mathbb{Z}^n$ and D is a real number.

- A linear term with coefficients given by the internal masses

$$\mathcal{L}(\underline{m}^2, \underline{x}) := \sum_{i=1}^n m_i^2 x_i + i\varepsilon \quad (2.6)$$

with ε a positive real number. We denote by $\underline{m}^2 := (m_1^2, \dots, m_n^2) \in \mathbb{C}^n$ the mass parameters.

The polynomials $\mathcal{U}(\underline{x})$ and $\mathcal{V}(\underline{s}, \underline{x})$ are determined by the Feynman graph Γ using graph theory, since the connection to graph theory will not be needed for the present work we refer to [28, 29, 30, 31]. We only list the main properties of these polynomials.

- $\mathcal{U}(\underline{x})$ is a homogeneous degree L polynomial in the variables $\underline{x} = (x_1, \dots, x_n)$ with coefficients in $\{0, 1\}$. It is at most linear in each of the x_i variables. This polynomial is determined by the homology of the vacuum graph and It does not depend on the kinematics parameters \underline{s} nor the masses \underline{m}^2 [28, 30].
- $\mathcal{V}(\underline{s}, \underline{x})$ is a homogeneous degree $L + 1$ polynomial in the variables x_1, \dots, x_n

$$\mathcal{V}(\underline{s}, \underline{x}) := \sum_{i=1}^{N_v} s_i V_i(\underline{x}) \quad (2.7)$$

where $V_i(\underline{x})$ is are homogeneous polynomials of degree $L + 1$ at most linear in each of the x_i variables with integer coefficients. We denote by $\underline{s} := (s_1, \dots, s_{N_v})$ the kinematic variables. The number of independent kinematic variables are constrained by the kinematic relations [32, 33]. These kinematic relations imply relations between the coefficients of the graph polynomial $\mathcal{V}(\underline{s}, \underline{x})$ affecting the singularity structure of integrand of the Feynman integral.

- The $i\varepsilon$ in (2.6) is the Feynman prescription for determining the contour of integration for the Feynman propagator. The integrals we will consider in this work exist in the limit $\varepsilon \rightarrow 0$ with $\varepsilon > 0$, and the differential equation derived in this work are independent of the value of ε , and we will set $\varepsilon = 0$. But for a proper definition of the Feynman integrals and a correct determination of the solution of the

derived differential equation one needs to reinstate the ε dependence. We refer to [34] for a recent throughout discussion.

2.2. Feynman integral as relative period integrals. — The integrand is a closed-form of the middle cohomology

$$\Omega_n(\underline{s}, \underline{m}^2; \nu, D; \underline{x}) \in H^{n-1}(\mathbb{P}^{n-1} \setminus X_\Gamma), \quad (2.8)$$

where X_Γ is the polar part of the Feynman integral in (2.1).

Bloch, Esnault, and Kreimer showed [9] that the Feynman integral is a period integral of the mixed Hodge structure

$$\mathfrak{M}(\Gamma) := H^{n-1}(\mathcal{P} \setminus \mathcal{X}, \mathcal{B} \setminus \mathcal{B} \cap \mathcal{X}; \mathbb{Q}). \quad (2.9)$$

We need to consider a blow-up in \mathbb{P}^{n-1} of linear space $f : \mathcal{P} \rightarrow \mathbb{P}^{n-1}$, such that all the vertices of Δ_n belong to $\mathcal{P} \setminus \mathcal{X}$ where \mathcal{X} is the strict transform of X_Γ . Let \mathcal{B} be the total inverse image of the coordinate simplex $\{x_1 x_2 \cdots x_n = 0 \mid [x_1, \dots, x_n] \in \mathbb{P}^{n-1}(\mathbb{R})\}$.

When all the mass parameters are non-vanishing $m_i^2 > 0$ for $1 \leq i \leq n$, the Feynman integral is absolutely convergent [35] when $\omega > 0$ in (2.5). The conditions for the absolute convergence of the Feynman integrals is a set of hyperplanes on the variables $(\underline{\nu}, D)$ in \mathbb{C}^{n+1} [36]. Because the polynomials $\mathcal{U}(\underline{x})$, $\mathcal{L}(\underline{m}^2, \underline{x})$ and $\mathcal{V}(\underline{s}, \underline{x})$ are independent of the dimension of space-time D and the exponents $\underline{\nu}$, the Feynman integral is a meromorphic function with singularities on linear hypersurfaces on $(\underline{\nu}, D)$ in \mathbb{C}^{n+1} as shown by [37] and reproved by Panzer in [3].

In the following we will only consider the case of convergent integrals with all non vanishing masses, i.e. $m_i \neq 0$ for $1 \leq i \leq n$ and $\omega > 0$.

We would like to identify the algebraic geometry behind the question of what kind of geometry is associated with the Feynman integral. The Feynman integrals are not periods of smooth hypersurfaces (except for some special cases like the two-loop sunset) and singularity structure of the integrand is rather non-trivial (but this makes the Feynman integrals so rich). One way to access a non-trivial information about the rank of the

Hodge structure is to perform a numerical evaluation of the periods and their associated Picard–Fuchs differential equations. From this information we can extract (an upper bound) on the dimension of the algebraic variety for which the Feynman integral is period integral.

2.3. Feynman integral differential equations. — The Feynman integrals are D-finite functions that satisfy finite order inhomogeneous differential equations with respect to their physical parameters [27, 38, 39, 40]. For a fixed loop order L and dimension D the space defined by all possible linear combinations of the Feynman integrals in (2.1)

$$V_\Gamma := \sum_{\underline{\nu} \in \mathbb{Z}^n} c_{\underline{\nu}}(D) I_\Gamma(\underline{s}, \underline{m}^2; \underline{\nu}, D) \quad (2.10)$$

is a finite dimensional vector space which dimension is given by the topological Euler characteristic of the complement of the vanishing locus of the \mathcal{U} and $\mathcal{F} = \mathcal{U}\mathcal{L} - \mathcal{V}$ polynomials [27]

$$\dim(V_\Gamma) = (-1)^{n+1} \chi((\mathbb{C}^*)^n \setminus \mathbb{V}(\mathcal{U}) \cup \mathbb{V}(\mathcal{F})), \quad (2.11)$$

where

$$\begin{aligned} \mathbb{V}(\mathcal{U}) &:= \{[x_1, \dots, x_n] \in \mathbb{P}^{n-1} \mid \mathcal{U}(\underline{x}) = 0\}; \\ \mathbb{V}(\mathcal{F}) &:= \{[x_1, \dots, x_n] \in \mathbb{P}^{n-1} \mid \mathcal{U}(\underline{x})\mathcal{L}(\underline{m}^2, \underline{x}) - \mathcal{V}(\underline{s}, \underline{x}) = 0\}. \end{aligned} \quad (2.12)$$

Since this vector space is finite-dimensional one can expand integral in the family of Feynman integrals $I_\Gamma(\underline{s}, \underline{m}^2; \underline{\nu}, D)$ on a basis of, so-called master integrals, $M_\Gamma(\underline{s})$ with coefficients given by rational functions of the parameters $\underline{s}, \underline{m}^2, \underline{\nu}$ and the dimension D .

Differentiating with respect to the physical parameters \underline{s} , the master integrals $M_\Gamma(\underline{s})$ satisfy the first order this differential system of equations (see [41] for a physicist’s review)

$$dM_\Gamma(\underline{s}) = A_\Gamma \wedge M_\Gamma(\underline{s}). \quad (2.13)$$

The matrix A_Γ is a flat connection satisfying

$$dA_\Gamma + A_\Gamma \wedge A_\Gamma = 0. \quad (2.14)$$

In positive integer dimension $D \in \mathbb{N}^*$ the connexion A_Γ is reducible and one important question is to obtain the minimal order differential equation acting on the Feynman integrals. This dimension in (2.10) gives an upper bound on the order of the minimal order differential operator acting on the Feynman integral.

Other approaches for deriving the system of differential operators acting on Feynman integrals used the GKZ toric approach [16, 25, 31, 42, 43, 44, 45], for constructing a D-module of differential operators from a toric formalism. But this approach fails to lead to the complete set of differential operators essentially because of the kinematic relations between the monomials in the graph polynomials.

The shortcomings of these approaches in providing directly a minimal order differential equation for Feynman integrals in integer dimensions, is the motivation of the present work.

2.4. Relations between various integrals. — We consider the action of the derivative with respect to the mass parameters

$$\frac{\partial}{\partial m_i^2} \left(\frac{\mathcal{U}(\underline{x})}{\mathcal{U}(\underline{x})\mathcal{L}(\underline{m}^2, \underline{x}) - \mathcal{V}(\underline{s}, \underline{x})} \right)^\omega = -\omega \left(\frac{\mathcal{U}(\underline{x})}{\mathcal{U}(\underline{x})\mathcal{L}(\underline{m}^2, \underline{x}) - \mathcal{V}(\underline{s}, \underline{x})} \right)^{\omega+1} x_i. \quad (2.15)$$

We then conclude that the derivative with respect to the mass parameter m_i^2 shifts the value of the $\underline{\nu}$ by $\underline{\nu}_i = (0, \dots, 0, 1, 0, \dots, 0)$ where the 1 is in the i th position. The anti-derivative (formal integration) with respect to the mass parameter

$$\partial_{m_i^2}^{-1} \left(\frac{\mathcal{U}(\underline{x})}{\mathcal{U}(\underline{x})\mathcal{L}(\underline{m}^2, \underline{x}) - \mathcal{V}(\underline{s}, \underline{x})} \right)^\omega = \frac{1}{\omega - 1} \left(\frac{\mathcal{U}(\underline{x})}{\mathcal{U}(\underline{x})\mathcal{L}(\underline{m}^2, \underline{x}) - \mathcal{V}(\underline{s}, \underline{x})} \right)^{\omega-1} x_i^{-1}. \quad (2.16)$$

Therefore we can restrict ourself to the case where $\underline{\nu} = (1, \dots, 1)$.

If one considers the differential operator $\mathcal{U}(\partial_{m_1^2}, \dots, \partial_{m_n^2})$ where the variable x_i is replaced by the partial derivative $\partial_{m_i^2}$ in the $\mathcal{U}(\underline{x})$ polynomial, we have

$$\mathcal{U}(\partial_{m_1^2}, \dots, \partial_{m_n^2})\Omega_n(\underline{s}, \underline{m}; \underline{\nu}, D, \underline{x}) = \prod_{r=0}^{L-1} (-(\omega + r))\Omega_n(\underline{s}, \underline{m}; \underline{\nu}, D - 2, \underline{x}) \quad (2.17)$$

and the operator when x_i are replaced by the $x_i^2 \partial_{m_i^2}^{-1}$ we have

$$\mathcal{U}(x_1^2 \partial_{m_1^2}^{-1}, \dots, x_n^2 \partial_{m_n^2}^{-1})\Omega(\underline{s}, \underline{m}; \underline{\nu}, D, \underline{x}) = \prod_{r=1}^L \frac{1}{\omega - r} \Omega(\underline{s}, \underline{m}; \underline{\nu}, D + 2, \underline{x}). \quad (2.18)$$

Such dimension shifting relations have been noticed by Tarasov [46] using a different setup.

3. Picard–Fuchs equations for Feynman integrals

From now we will focus on the case where $\underline{\nu} = (1, \dots, 1)$, so that

$$\Omega(t; D, \underline{x}) := \left(\frac{\mathcal{U}(\underline{x})}{\mathcal{U}(\underline{x})\mathcal{L}(\underline{m}^2, \underline{x}) - t\mathcal{V}(\underline{s}, \underline{x})} \right)^{n - \frac{LD}{2}} \frac{\Omega_0^{(n)}}{\mathcal{U}(\underline{x})^{\frac{D}{2}}}. \quad (3.1)$$

We consider the case of $D = 2$ and $D = 4$ dimensions so that we have a rational differential form in $\mathbb{P}^{n-1}(x_1, \dots, x_n)$, and convergent integral when integrating this differential form over the positive orthant. We have chosen to consider the variation with respect to the parameter t as an overall scale in front of the kinematics graph polynomial $\mathcal{V}(\underline{s}, \underline{x})$. One can consider a variation with respect to any other physical parameter amongst the masses m_i^2 variable or any independent kinematics s_i variable. In that case the denominator would take the form $\mathcal{F}_0(\underline{x}) + t\mathcal{F}_1(\underline{x})$. Clearly different choices for the parameters t amongst the kinematic or mass parameters, will lead to different differential equations. But for generic values of the physical parameters, we conjecture that they all

arise from the same (singular) geometry determined by the singularities locus of the integrand (3.1).

We will derive the Picard–Fuchs operator differential operator

$$\mathcal{L}_t = \sum_{r=0}^{o_i} q_r(\underline{m}, \underline{s}; t) \left(\frac{d}{dt} \right)^r \quad (3.2)$$

such that $\mathcal{L}_t \Omega(t; D, \underline{x}) = d\beta(\underline{x}, t)$, for some holomorphic $n-1$ -form $\beta(\underline{x}, t)$ on $\mathbb{P}^{n-1} \setminus X_\Gamma$, corresponding to the certificate in (1.4).

Given any n -cycle γ in $\mathbb{P}^{n-1} \setminus X_\Gamma$, we obtain that

$$\mathcal{L}_t \int_\gamma \Omega(t; D, \underline{x}) = 0, \quad (3.3)$$

so that \mathcal{L}_t is a differential equation satisfied by the period integral defined by the integration of the differential form over a cycle.

In the construction we will only consider the case where $\beta(\underline{x}, t)$ is holomorphic on $\mathbb{P}^{n-1} \setminus X_\Gamma$, that is $\beta(\underline{x}, t)$ does not have poles that are not present in $\Omega(t; D, \underline{x})$. When $\beta(\underline{x}, t)$ is only meromorphic, the left-hand side in (3.3) may not vanish after integration on γ .

Consider the rational function

$$F(x_1, x_2) = \frac{ax_1 + bx_2 + c}{(\alpha x_1^2 + \beta x_2^2 + \gamma x_1 x_2 + \delta x_1 + \eta x_2 + \zeta)^2} \quad (3.4)$$

where $a, b, c, \alpha, \beta, \gamma, \delta, \eta, \zeta$ are independent of x_1 and x_2 (this is the generic form of the multi-loop ice-cream integrand studied in section 5.) Using the creative telescoping algorithm [47, 48] we find that

$$F(x_1, x_2) = \partial_{x_1} \frac{N_1(x_1, x_2)}{D_1(x_1, x_2)} + \partial_{x_2} \frac{N_2(x_1, x_2)}{D_2(x_1, x_2)} \quad (3.5)$$

where $N_i(x_1, x_2)$ with $i = 1, 2$ are polynomials in x_1 and x_2 and the denominator is (the coefficients are given on this page [identity](#))

$$\begin{aligned} D_1(x_1, x_2) &= D_2(x_1, x_2) (x_2(2\alpha b - a\gamma) - a\delta + 2\alpha c), \\ D_2(x_1, x_2) &= 2 \left(4\alpha\beta\zeta - \alpha\epsilon^2 - \beta\delta^2 - \gamma^2\zeta + \gamma\delta\epsilon \right) (x_2(2\alpha b - a\gamma) - a\delta + 2\alpha c) \\ &\quad \times \left(\alpha x_1^2 + \beta x_2^2 + \gamma x_1 x_2 + \delta x_1 + \eta x_2 + \zeta \right)^2. \end{aligned} \quad (3.6)$$

The denominator on the right-hand-side has a pole at $x_2^0 = (a\delta - 2\alpha c)/(2\alpha b - a\gamma)$ which is not a pole of the original function. This means one can find a cycle where γ passing by x_2^0 . Since $F(x_1, x_2)$ has no pole at $x_2 = x_2^0$ the integral of $\int_\gamma F(x_1, x_2)$ is finite and non-vanishing. Therefore, the certificat cannot have poles that are not poles of the original function. Examples of this phenomenon were given by Picard [49] (see also [48]).

We will use the factorisation algorithm in [23] to certify whether the Picard–Fuchs operator is irreducible or not. Irreducibility implies that the operator is minimal. The converse does not hold, the minimal annihilating operator of a given function maybe reducible. We encounter this complication for the Kite graph in four dimensions in section ??.

3.1. The Griffiths–Dwork reduction. — The Griffiths–Dwork reduction is the main tool for computing Picard–Fuchs differential equations [50, 51, 52], although it needs to be completed by other reductions rules with the projective hypersurface X_Γ is singular. This section describes briefly this reduction and its extension, following [26].

For a given D , let us write $\Omega(t; D, \underline{x})$ as $\frac{A(\underline{x})\Omega_0}{P(\underline{x})^k}$, where A and P are homogeneous polynomial in \underline{x} whose coefficients are rational functions in t . We assume moreover that P is square-free (as a polynomial in \underline{x}).

It makes the computation easier to reformulate the integral in \mathbb{P}^{n-1} over an $n - 1$ -cycle γ as an integral in \mathbb{C}^n over the n -cycle $\tilde{\gamma} = \{\underline{x} \in \mathbb{C}^n \mid [\underline{x}] \in \gamma \text{ and } \|\underline{x}\| = 1\}$:

$$\int_\gamma \frac{A(\underline{x})\Omega_0}{P(\underline{x})^k} = \frac{1}{2\pi i} \int_{\tilde{\gamma}} \frac{A(\underline{x})}{P(\underline{x})^k} d\underline{x}, \quad (3.7)$$

where $d\underline{x} = dx_1 \cdots dx_n$.

Assume that A is in the Jacobian ideal of P , that is $A = C_1 \frac{\partial P}{\partial x_1} + \cdots + C_n \frac{\partial P}{\partial x_n}$ for some homogeneous polynomials C_i . Then we can write

$$Ad\underline{x} = dP \wedge (C_1 \xi_1 + \cdots + C_n \xi_n), \quad (3.8)$$

where $\xi_i = (-1)^{i-1} dx_1 \cdots \widehat{dx_i} \cdots dx_n$. Note that $d\xi_i = dx_1 \cdots dx_n$, so

$$(k-1) \frac{A}{P^k} d\underline{x} = \frac{\sum_i \frac{\partial C_i}{\partial x_i}}{P^{k-1}} d\underline{x} - d \left(\sum_i \frac{C_i}{P^{k-1}} \xi_i \right). \quad (3.9)$$

The integral on $\tilde{\gamma}$ of the exact differential vanishes, because we assume that P does not vanish on $\tilde{\gamma}$, so, assuming $k > 1$, we obtain that

$$\int_{\tilde{\gamma}} \frac{A(\underline{x})}{P(\underline{x})^k} d\underline{x} = -\frac{1}{k-1} \int_{\tilde{\gamma}} \frac{\sum_i \frac{\partial C_i}{\partial x_i}}{P^{k-1}} d\underline{x}. \quad (3.10)$$

The left-hand side is the integral of a form with pole order k , while the right-hand side has pole order $k-1$. In the general case, when A is not in the Jacobian ideal, we may compute a normal form $R(\underline{x})$ of A modulo the Jacobian ideal (using for example a Gröbner basis) that is

$$A = R + C_1 \frac{\partial P}{\partial x_1} + \cdots + C_n \frac{\partial P}{\partial x_n}, \quad (3.11)$$

with the property that R depends only on the class of A modulo the Jacobian ideal. Then we have

$$\int_{\tilde{\gamma}} \frac{A(\underline{x})}{P(\underline{x})^k} d\underline{x} = \int_{\tilde{\gamma}} \frac{R(\underline{x})}{P(\underline{x})^k} d\underline{x} - \frac{1}{k-1} \int_{\tilde{\gamma}} \frac{\sum_i \frac{\partial C_i}{\partial x_i}}{P^{k-1}} d\underline{x}. \quad (3.12)$$

The right-hand side is made of a term with a pole order k but reduced numerator, and a term with pole order $k-1$, to which we can apply the procedure recursively. In the end, we obtain a decomposition

$$\int_{\tilde{\gamma}} \frac{A(\underline{x})}{P(\underline{x})^k} d\underline{x} = \sum_{i=1}^k \int_{\tilde{\gamma}} \frac{R_i(\underline{x})}{P(\underline{x})^i} d\underline{x}, \quad (3.13)$$

for some polynomials $R_i(\underline{x})$ in normal form with respect to the Jacobian ideal. Moreover, R_i is homogeneous of degree $\deg R_i = i \deg P - n$.

3.2. Picard–Fuchs equations in the smooth case. — In the case where the hypersurface $X_\Gamma \subset \mathbb{P}^{n-1}$ is smooth, the Jacobian ideal contains all the homogeneous polynomials of degree at least $n(\deg P - 1) - n + 1$ (this is the Macaulay bound) this implies in particular that in the

decomposition (3.13), the polynomial R_i with $i \geq n$ are all zero. This gives the following algorithm to compute the Picard–Fuchs equation.

We compute the Griffiths–Dwork decomposition of the j th derivative (with respect to t) of the integral $I(t) = \int_{\tilde{\gamma}} \frac{A(\underline{x})}{P(\underline{x})^k} d\underline{x}$ as

$$\frac{d^j I}{dt^j} = \int_{\tilde{\gamma}} \frac{A_j(\underline{x})}{P(\underline{x})^{k+i}} d\underline{x} = \sum_{i=1}^{n-1} \int_{\tilde{\gamma}} \frac{R_{ji}(\underline{x})}{P(\underline{x})^i} d\underline{x}, \quad (3.14)$$

where A_j is a homogeneous polynomial (of degree $(k+i) \deg P - n$) and the R_{ji} are homogeneous polynomials of degree $i \deg P - n$. The first equality is obtained by differentiating under the integral sign, and the second equality is the Griffiths–Dwork reduction.

In view of the degree constraint on the polynomials R_{ji} , the tuples $(R_{j1}, \dots, R_{j,n-1})$, for $j \geq 0$, lie in a finite dimensional vector space over the base field $\mathbb{C}(t)$. Given a N which exceeds this dimension, we can therefore compute coefficients $a_i(t) \in \mathbb{C}(t)$, not all zero, such that

$$a_N(t) \frac{d^N I}{dt^N} + \dots + a_1(t) \frac{dI}{dt} + a_0(t) I(t) = 0, \quad (3.15)$$

which is the desired differential equation, simply by computing a non vanishing solution of the linear system

$$\sum_{j=0}^N a_j(t) R_{ji}(t; \underline{x}) = 0, \quad 1 \leq i \leq n, \quad (3.16)$$

with unknowns a_0, \dots, a_N .

3.3. An extension of the Griffiths–Dwork reduction. — When the hypersurface $X_\Gamma \subset \mathbb{P}^{n-1}$ is not smooth, the Griffiths–Dwork reduction step (3.12) may not be enough to reduce the pole order when $k \geq n$, independently on the numerator. Other reduction rules come from the syzygies of the derivatives $\frac{\partial P}{\partial x_i}$. Let B_1, \dots, B_n be homogeneous of degree $k \deg P - n + 1$ such that $\sum_i B_i \frac{\partial P}{\partial x_i} = 0$. The tuple (B_1, \dots, B_n) is

called a *syzygy*. The same computation as for (3.9) shows that

$$\frac{\sum_i \frac{\partial B_i}{\partial x_i}}{P^k} d\underline{x} = d \left(\sum_i \frac{B_i}{P^k} \xi_i \right), \quad (3.17)$$

so that

$$\int_{\tilde{\gamma}} \frac{\sum_i \frac{\partial B_i}{\partial x_i}}{P^k} d\underline{x} = 0. \quad (3.18)$$

In singular cases, these relations are missed by the Griffiths–Dwork reduction.

A syzygy (B_1, \dots, B_n) is a *trivial* syzygy if there are polynomials D_{ij} such that $D_{ij} = -D_{ji}$ and such that $B_i = \sum_{j=1}^n D_{ij} \frac{\partial P}{\partial x_j}$, (which implies immediately the relation $\sum_i B_i \frac{\partial P}{\partial x_i} = 0$). Trivial syzygies are irrelevant because the corresponding relations are already reduced by the Griffiths–Dwork reduction. Indeed, the numerator $\sum_i \frac{\partial B_i}{\partial x_i}$ in (3.17) is in the Jacobian ideal:

$$\sum_i \frac{\partial B_i}{\partial x_i} = \underbrace{\sum_i \sum_j D_{ij} \frac{\partial^2 P}{\partial x_j \partial x_i}}_{=0} + \sum_j \left(\sum_i \frac{\partial D_{ij}}{\partial x_i} \right) \frac{\partial P}{\partial x_j}. \quad (3.19)$$

This leads to the following extension of the Griffiths–Dwork reduction. Given a form $\frac{A}{P^k} \underline{x}$, with A homogeneous of degree $k \deg P - n$, we first compute a basis of the space S_k of all syzygies of degree $k \deg P - n + 1$ quotiented by the space of trivial syzygies. Then we compute a normal form R of A modulo the Jacobian ideal plus the space $dV = \left\{ \sum_i \frac{\partial B_i}{\partial x_i} \mid \underline{B} \in V \right\}$, that is

$$A = R + \underbrace{\sum_i \frac{\partial B_i}{\partial x_i}}_{\in dV} + \underbrace{C_1 \frac{\partial P}{\partial x_1} + \dots + C_n \frac{\partial P}{\partial x_n}}_{\in \text{Jacobian ideal}}, \quad (3.20)$$

for some polynomials B_i and C_i . This leads to the following relation, similar to (3.9),

$$(k-1) \frac{A}{P^k} d\underline{x} = \frac{\sum_i \frac{\partial C_i}{\partial x_i}}{P^{k-1}} d\underline{x} - d \left(\sum_i \frac{B_i}{P^k} \xi_i + \sum_i \frac{C_i}{P^{k-1}} \xi_i \right). \quad (3.21)$$

The integral on $\tilde{\gamma}$ of the exact differential vanishes, so, assuming $k > 1$, we obtain that

$$\int_{\tilde{\gamma}} \frac{A(\underline{x})}{P(\underline{x})^k} d\underline{x} = -\frac{1}{k-1} \int_{\tilde{\gamma}} \frac{\sum_i \frac{\partial C_i}{\partial x_i}}{P^{k-1}} d\underline{x}, \quad (3.22)$$

exactly similar to (3.10). We can apply the same reduction procedure to the right-hand side, by induction on the pole order. Then we compute Picard–Fuchs differential equations in the same way as in the smooth case.

The extended Griffiths–Dwork reduction presented above is not always enough and may need further extensions. There is a hierarchy of extensions which eventually collapse to the strongest possible reduction. However, for all the computations presented here, we only needed the first extension.

4. The multiloop sunset graphs

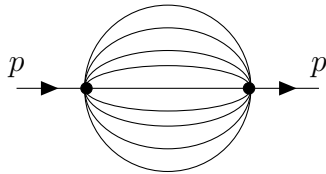


FIGURE 4.1. Multi-loop sunset

The multiloop sunset graphs are two-point graphs connected by n edges as depicted in figure 4.1. In two dimensions, the associated differential form in $\mathbb{P}^{n-1}(x_1, \dots, x_n)$ is given by

$$\Omega_n^\ominus(t, \underline{m}^2) := \frac{\Omega_0^{(n)}}{\mathcal{F}_n^\ominus(t, \underline{m}^2; \underline{x})} \quad (4.1)$$

with $\Omega_0^{(n)}$ the natural projective form on \mathbb{P}^{n-1} defined in (2.4) and the degree n homogeneous polynomial

$$\mathcal{F}_n^\ominus(t, \underline{m}^2; \underline{x}) := x_1 \cdots x_n \left(\left(\sum_{i=1}^n \frac{1}{x_i} \right) \left(\sum_{j=1}^n m_j^2 x_j \right) - t \right). \quad (4.2)$$

We seek a minimal order differential operator

$$\mathcal{L}_t = \sum_{r=0}^{\infty} q_r(t, \underline{m}^2) \left(\frac{d}{dt} \right)^r \quad (4.3)$$

where $q_r(t, \underline{m}^2)$ is a polynomial in t such that

$$\mathcal{L}_t \Omega_n^\ominus(t, \underline{m}^2) = d\beta(t, \underline{m}^2). \quad (4.4)$$

For $n \geq 4$ the Jacobian ideal $J = \langle \partial_{x_r} \mathcal{F}_n^\ominus(t, \underline{m}^2; \underline{x}), 1 \leq r \leq n \rangle$ has non-isolated singularities at the positions

$$x_i = x_j = 0, \quad \sum_{\substack{1 \leq r \leq n \\ r \neq i, r \neq j}} m_r^2 x_r = 0. \quad (4.5)$$

Therefore we need to apply the Griffiths–Dwork reduction adapted to this case as described in section 3.1.

The equation $\mathcal{F}_n^\ominus(t, \underline{m}^2; \underline{x})$ defines families of Calabi–Yau manifolds associated to the root lattice A_n studied by Verrill [53]. In this case the denominator of period integral takes the form of $t - \phi_n(x_1, \dots, x_n)$ where $\phi_n(\underline{x})$ is a Laurent polynomial. The period integrals associated to Laurent polynomials are connected to mirror symmetry for Fano manifolds [54, 55, 56], and our analysis gives supplementary support that the $n - 1$ -loop sunset Feynman integrals are relative periods of (singular) Calabi–Yau of dimension complex dimension $n - 2$ [11, 11, 14, 17, 18, 20, 57, 58, 59].

Conjecture 4.1 (Order of the sunset Picard–Fuchs operator)

The order of the minimal order Picard–Fuchs operator for generic

mass parameters is

$$o_n = 2^n - \binom{n+1}{\lfloor \frac{n+1}{2} \rfloor}; n \geq 2. \quad (4.6)$$

The coefficient of the highest order derivative reads

$$q_{o_n}(t, \underline{m}^2) = t^{\alpha(n)} \prod_{i=1}^{|\mu_n|} (t - \mu_n^i) \tilde{q}_{o_n}(t) \quad (4.7)$$

where $\alpha(n) \in \mathbb{N}$. The polynomial $\tilde{q}_{o_n}(t)$ contains the apparent singularities, and the non apparent singularities are located at $t = 0$ and $t = \mu_n$ which are the 2^n so-called thresholds

$$\mu_n = \left\{ \left(\sum_{i=1}^n \epsilon_i m_i \right)^2, (\epsilon_1, \dots, \epsilon_n) \in \{-1, 1\}^n \right\}. \quad (4.8)$$

where only distinct values of the squares are kept.

- For $n = 2$ this is shown in section 4.1
- For $n = 3$ this is shown section 4.2
- For $n = 4$ this is shown section 4.3
- For $n = 5$ this is shown section 4.4
- For $n = 6$ this is shown section 4.5
- For $n = 7$ the algorithm gives an upper bound on the order of the differential operator matching the value o_6 , see section 4.6.

When all the mass parameters are identified $m_1^2 = \dots = m_n^2$ the thresholds in (4.8) are located at the positions

$$\mu_n = \begin{cases} \{0, 2^2, \dots, n^2\} & \text{for } n \equiv 0 \pmod{2} \\ \{1, 3^2, \dots, n^2\} & \text{for } n \equiv 1 \pmod{2} \end{cases} \quad (4.9)$$

and the minimal order differential operator in two-dimensions has of order $n - 1$ and its form is given by [22]

$$\begin{aligned} q_{n-1}(t) &= t^{\lceil \frac{n}{2} \rceil + \frac{(-1)^{n-1} + 1}{2}} \prod_{i=0}^{\lfloor \frac{n}{2} \rfloor} (t - (n - 2i)^2) \\ q_{n-2}(t) &= \frac{n-1}{2} \frac{dq_{n-1}(t)}{dt} \\ q_0(t) &= t - n \end{aligned} \tag{4.10}$$

Generalisation to higher dimensions has been obtained in [16, 17, 18, 60, 61]. In section 4.3 and 4.4 we will show how the restriction of the masses leads to the factorisation of the differential operator at three- and four-loop orders respectively.

The certificate Q in (1.5) or the $d\beta$ in (4.4) leads to huge expressions that are evaluated by the algorithm, since they assure that the telescoper annihilates the integrand but we will not consider them in this work. Our results are statements about the Picard–Fuchs operator for the period integral defined by the integration over a cycle. In the case of the sunset graph the integral over the torus has the large- t series expansion (this is the so-called maximal cut discussed in [24])

$$\pi_n^\ominus(t) = \int_{|x_1|=1 \dots = |x_n|=1} \Omega_n^\ominus(t) = \sum_{m \geq 0} t^{-m-1} \sum_{\substack{r_1 + \dots + r_m = m \\ r_i \geq 0}} \left(\frac{m!}{r_1! \dots r_m!} \right)^2. \tag{4.11}$$

The minimal order differential operator is this annihilator of this series expansion $\mathcal{L}_t^n \pi_n^\ominus(t) = 0$.

4.1. One-loop sunset. — In this section we recall the results for the Picard–Fuchs operators for the one-loop loop sunset integral

$$\Omega_2^\ominus(t, \underline{m}^2) = \frac{\Omega_0^{(2)}}{\mathcal{F}_2^\ominus(t, \underline{m}^2; \underline{x})} \tag{4.12}$$

with

$$\mathcal{F}_2^\ominus(t, \underline{m}^2; \underline{x}) = tx_1x_2 - (m_1^2x_1 + m_2^2x_2) \left(\frac{1}{x_1} + \frac{1}{x_2} \right) x_1x_2. \quad (4.13)$$

The differential operator is readily obtained by applying the Griffiths–Dwork reduction (see [25]) to get⁽²⁾

$$\mathcal{L}_t^{[1^2]} = (t - (m_1 + m_2)^2)(t - (m_1 - m_2)^2) \frac{d}{dt} + t - m_1^2 - m_2^2. \quad (4.14)$$

The certificate has

$$Q_1 = 2m_2^2x_2; \quad Q_2 = -(m_1^2 + m_2^2 - p^2)x_2 \quad (4.15)$$

so that

$$\mathcal{L}_t^{[1^2]} \frac{1}{\mathcal{F}_2^\ominus(t, \underline{m}^2; \underline{x})} + \sum_{i=1}^2 \frac{\partial}{\partial x_i} Q_i \frac{1}{\mathcal{F}_2^\ominus(t, \underline{m}^2; \underline{x})} = 0. \quad (4.16)$$

4.2. Two-loop sunset. — In this section we recall the results for the Picard–Fuchs operators for the two-loop sunset integral

$$\Omega_3^\ominus(t, \underline{m}^2) = \frac{\Omega_0^{(3)}}{\mathcal{F}_3^\ominus(t, \underline{m}^2; \underline{x})} \quad (4.17)$$

with

$$\mathcal{F}_3^\ominus(t, \underline{m}^2; \underline{x}) = tx_1 \cdots x_3 - (m_1^2x_1 + \cdots + m_3^2x_3) \left(\frac{1}{x_1} + \cdots + \frac{1}{x_3} \right) x_1 \cdots x_3. \quad (4.18)$$

In this case the singular locus of the differential form defines a smooth elliptic curve in \mathbb{P}^2

$$\sum_{i=1}^3 x_i^{-1} \sum_{j=1}^3 m_j^2 x_j - t = 0. \quad (4.19)$$

⁽²⁾The superscript denotes the number of independent mass parameter. When the mass parameters are identified with s different values, we use the notation $[r_1^{a_1} r_2^{a_2} \cdots r_s^{a_s}]$ such that $\sum_{i=1}^s a_i r_i = n$. When all the masses parameters are different $m_1 \neq \cdots \neq m_n$ we use $[1^n]$.

The Picard–Fuchs operator can be derived by applying the Griffiths–Dwork reduction method [12, 25, 62] giving the second order operator

$$\mathcal{L}_t^{[1^3]} = \sum_{r=0}^2 q_r(t, \underline{m}^2) \left(\frac{d}{dt} \right)^r. \quad (4.20)$$

The coefficients are polynomials in t of degree $5 + r$ with $0 \leq r \leq 2$ are listed on this page [2sunset](#). The coefficient of the highest derivative term is given by

$$\begin{aligned} q_2(t, \underline{m}^2) &= t \prod_{i=1}^4 (t - \mu_3^i) \\ &\times ((m_1^2 + m_2^2 + m_3^2)^2 - 4(m_1^2 m_2^2 + m_1^2 m_3^2 + m_2^2 m_3^2) + 2(m_1^2 + m_2^2 + m_3^2)t - 3t^2) \end{aligned} \quad (4.21)$$

where we have introduced the thresholds contributions

$$\mu_3 := \{(-m_1 + m_2 + m_3)^2, (m_1 - m_2 + m_3)^2, (m_1 + m_2 - m_3)^2, (m_1 + m_2 + m_3)^2\}. \quad (4.22)$$

which are the position of the regular singularities. The roots of the polynomial in the second line are apparent singularities.

4.3. Three-loop sunset. — In this section we give the results for the Picard–Fuchs operators for the three-loop loop sunset integral

$$\Omega_4^\ominus(t, \underline{m}^2) = \frac{\Omega_0^{(4)}}{\mathcal{F}_4(t, \underline{m}^2; \underline{x})} \quad (4.23)$$

with

$$\mathcal{F}_4^\ominus(t, \underline{m}^2; \underline{x}) = tx_1 \cdots x_4 - (m_1^2 x_1 + \cdots + m_4^2 x_4) \left(\frac{1}{x_1} + \cdots + \frac{1}{x_4} \right) x_1 \cdots x_4. \quad (4.24)$$

We list the properties of the Picard–Fuchs operators for all the mass configurations. The expressions are accessible at the online at [3sunset](#)

– **The four masses case** $m_1 \neq m_2 \neq m_3 \neq m_4$ **labelled** [1⁴]:

When all the internal masses are different and all non-vanishing the

Picard–Fuchs operator is of order 6

$$\mathcal{L}_t^{[1^4]} = \sum_{r=0}^6 q_r^{[1^4]}(t, \underline{m}^2) \left(\frac{d}{dt} \right)^r. \quad (4.25)$$

the coefficients $q_r^{[1^4]}(t, \underline{m}^2)$ is polynomials in t of degree $21 + r$ for $0 \leq r \leq 6$.⁽³⁾ The coefficient of the highest order operator is

$$q_6^{[1^4]}(t, \underline{m}^2) = (t) \prod_{i=1}^8 (t - (\mu_i^{(4)})^2) \tilde{q}_6^{[1^4]}(t, \underline{m}^2) \quad (4.26)$$

with the thresholds contributions corresponding

$$\begin{aligned} \{\mu_i^{(4)}\} := & \left\{ (m_1 + m_2 + m_3 + m_4)^2, (m_1 + m_2 + m_3 - m_4)^2, \right. \\ & (m_1 + m_2 - m_3 + m_4)^2, (m_1 + m_2 - m_3 - m_4)^2, \\ & (m_1 - m_2 + m_3 + m_4)^2, (m_1 - m_2 + m_3 - m_4)^2, \\ & \left. (m_1 - m_2 - m_3 + m_4)^2, (-m_1 + m_2 + m_3 + m_4)^2 \right\} \quad (4.27) \end{aligned}$$

and where $\tilde{q}_6^{[1^4]}(t, \underline{m}^2)$ is an degree 17 polynomial in t .

The differential equation has only regular singularities⁽⁴⁾ located at

$$t = 0, \infty, (\mu_i^{(4)})^2 \quad 1 \leq i \leq 8, \quad (4.28)$$

and the apparent singularities at the roots of a degree 17 polynomial $\tilde{q}_6^{[1^4]}(t, \underline{m}^2)$.

- **The three masses case** $m_1 \neq m_2 \neq m_3 = m_4$ **labelled** [1²2]: the Picard–Fuchs operator of order 5

$$\mathcal{L}_t^{[1^2 2]} = \sum_{r=0}^5 q_r^{[1^2 2]}(t, \underline{m}^2) \left(\frac{d}{dt} \right)^r, \quad (4.29)$$

⁽³⁾For all the Picard–Fuchs operator considered in this work the degree refers to the degree in t of the polynomial multiplying the higher order derivative term. By homogeneity the degree of the polynomial coefficient decrease with the derivative order.

⁽⁴⁾the position of singular fibres of the pencil of $K3$ surfaces (see the discussion in [63] and [58])

the coefficients $q_r^{[122]}(t, \underline{m}^2)$ is polynomials in t of degree $12 + r$ for $0 \leq r \leq 5$.

- **The two masses case** $m_1 = m_2 \neq m_3 = m_4$ **labelled** [22]: The Picard–Fuchs operator of order 4

$$\mathcal{L}_t^{[22]} = \sum_{r=0}^4 q_r^{[22]}(t, \underline{m}^2) \left(\frac{d}{dt} \right)^r, \quad (4.30)$$

the coefficients $q_r^{[22]}(t, \underline{m}^2)$ is polynomials in t of degree $6 + r$ for $0 \leq r \leq 4$.

- **The two masses case** $m_1 \neq m_2 = m_3 = m_4$ **labelled** [13]: The Picard–Fuchs operator of order 4

$$\mathcal{L}_t^{[13]} = \sum_{r=0}^4 q_r^{[122]}(t, \underline{m}^2) \left(\frac{d}{dt} \right)^r, \quad (4.31)$$

the coefficients $q_r^{[13]}(t, \underline{m}^2)$ is polynomials in t of degree $5 + r$ for $0 \leq r \leq 4$.

- **The single mass case** $m_1 = m_2 = m_3 = m_4$ **labelled** [4]: The Picard–Fuchs operator of order 3

$$\mathcal{L}_t^{[4]} = \sum_{r=0}^5 q_r^{[3]}(t, \underline{m}^2) \left(\frac{d}{dt} \right)^r. \quad (4.32)$$

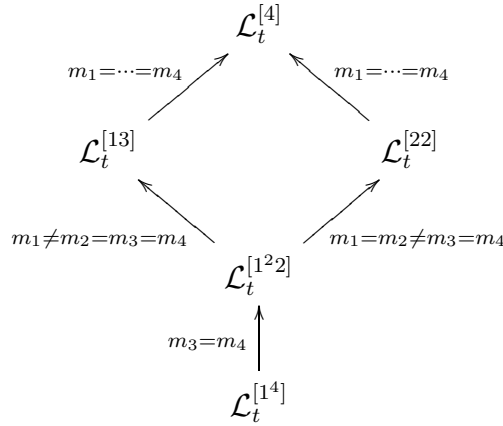
the coefficients $q_r^{[4]}(t, \underline{m}^2)$ is polynomials in t of degree $1 + r$ for $0 \leq r \leq 3$. The Picard–Fuchs operator was derived in [11, 22, 53, 64]. It was shown in these references that this third order Picard–Fuchs operator is the symmetric square of the second order differential operator

$$\mathcal{L}_t^{[3]} = \frac{t - 8m_1^2}{4t(t - 4m_1^2)(t - 16m_1^2)} + \frac{2(32m_1^2 - 15m_1t + t^2)}{t(t - 4m_1^2)(t - 16m_1^2)} \left(\frac{d}{dt} \right) + \left(\frac{d}{dt} \right)^2 \quad (4.33)$$

which is all equal mass Picard–Fuchs operator for the two-loop sunset after the change of variables $t \rightarrow 4m_1^2 - \frac{(t-3m_1^2)^2}{t}$ and the rescaling $f(t) \rightarrow \sqrt{t}f(t)$.

4.3.1. Mass specialisation. — The Picard–Fuchs operator for the different mass configurations have been derived using the extension of the Griffith–Dwork reduction presented in section 3.3.

We analyse the relation between these different Picard–Fuchs operators. When some masses are identified the order of the Picard–Fuchs operator decreases. By specialising the mass parameters the Picard–Fuchs operator becomes reducible as represented on this diagram



The arrows $P^a \rightarrow P^b$ represent the left factorisation of the differential operator P^a , so that the operator P^b divides the operator P^a . The factorisation can be obtained using Maple DEtools package or the factorisation algorithm [23]. The page 3sunset contains illustrative examples.

We note that the certificate $d\beta$ factorises in a similar way, and starting from the general four mass differential operator one can derive all the special masses cases.

4.4. The four-loop sunset. — In this section we give the result for the Picard–Fuchs operators for the four-loop loop sunset integral

$$\Omega_5^\ominus(t, \underline{m}^2) = \frac{\Omega_0^{(5)}}{\mathcal{F}_5^\ominus(t, \underline{m}^2; \underline{x})} \quad (4.34)$$

with

$$\mathcal{F}_5^\ominus(t, \underline{m}^2; \underline{x}) = tx_1 \cdots x_5 - (m_1^2 x_1 + \cdots + m_5^2 x_5) \left(\frac{1}{x_1} + \cdots + \frac{1}{x_5} \right) x_1 \cdots x_5. \quad (4.35)$$

We list the properties of the Picard–Fuchs operators for all the mass configurations. The expressions for the coefficients are accessible at the online at [4sunset](#).

- **The five masses are different** $m_1 \neq m_2 \neq m_3 \neq m_4 \neq m_5$ **and all non-vanishing configuration:** the Picard–Fuchs operator is of order 12

$$\mathcal{L}_t^{[15]} = \sum_{r=0}^{12} q_r^{[15]}(t, \underline{m}^2) \left(\frac{d}{dt} \right)^r. \quad (4.36)$$

the coefficients $q_r^{[15]}(t, \underline{m}^2)$ is polynomials in t of degree $109 + r$ for $0 \leq r \leq 12$. The coefficient $q_{12}^{[15]}(t, \underline{m}^2)$ has the following form

$$q_{12}^{[15]}(t, \underline{m}^2) = (t)^{12} \prod_{i=1}^{16} (t - \mu_i^2) \tilde{q}_{12}^{[15]}(t, \underline{m}^2) \quad (4.37)$$

where $\tilde{q}_{12}^{[15]}(t, \underline{m}^2)$ is a degree 98 polynomial in t , and the μ_i are the 16 thresholds

$$\begin{aligned} \{\mu_i\} := & \left\{ (m_1 + m_2 + m_3 + m_4 + m_5)^2, (m_1 + m_2 + m_3 + m_4 - m_5)^2, \right. \\ & (m_1 + m_2 + m_3 - m_4 + m_5)^2, (m_1 + m_2 + m_3 - m_4 - m_5)^2, (m_1 + m_2 - m_3 + m_4 + m_5)^2, \\ & (m_1 + m_2 - m_3 + m_4 - m_5)^2, (m_1 + m_2 - m_3 - m_4 + m_5)^2, (-m_1 - m_2 + m_3 + m_4 + m_5)^2, \\ & (m_1 - m_2 + m_3 + m_4 + m_5)^2, (m_1 - m_2 + m_3 + m_4 - m_5)^2, (m_1 - m_2 + m_3 - m_4 + m_5)^2, \\ & (-m_1 + m_2 - m_3 + m_4 + m_5)^2, (m_1 - m_2 - m_3 + m_4 + m_5)^2, (-m_1 + m_2 + m_3 - m_4 + m_5)^2, \\ & \left. (-m_1 + m_2 + m_3 + m_4 - m_5)^2, (-m_1 + m_2 + m_3 + m_4 + m_5)^2 \right\} \quad (4.38) \end{aligned}$$

The differential equation has only regular singularities located⁽⁵⁾

$$t = 0, \infty, \mu_i \quad 1 \leq i \leq 16, \quad (4.39)$$

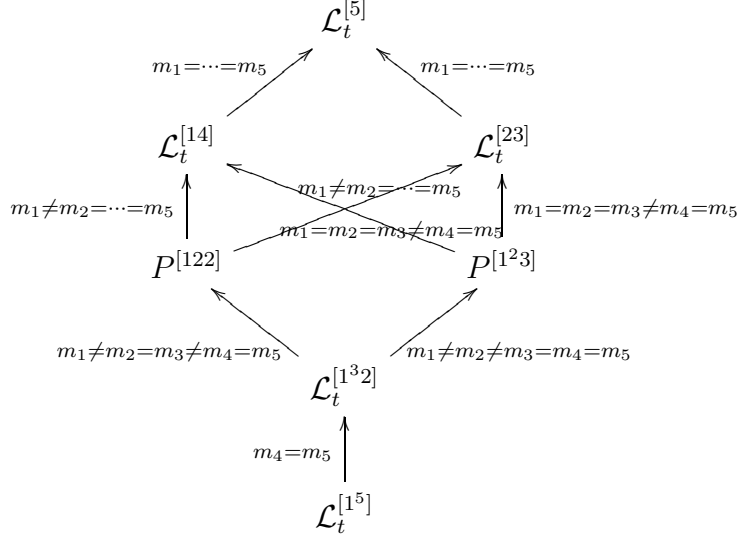
⁽⁵⁾They correspond to the positions of singular fibres of the pencil of Calabi–Yau three-fold (see the discussion in [63] and [58])

and the apparent singularities at the roots of the degree 98 polynomial $\tilde{q}_{12}^{[1^5]}(t, \underline{m}^2)$.

- **The four different mass configuration** $m_1^2 \neq m_2^2 \neq m_3^2 \neq m_4^2 = m_5$ The differential operator has order 10. The degree of the polynomial coefficient $q_r^{[1^4]}(t, \underline{m}^2)$ are $57 + r$ with $0 \leq r \leq 10$.
- **The three different mass configuration:** the differential operator has order 8.
 - $m_1 \neq m_2 \neq m_3 = m_4 = m_5$: the degree of the polynomial coefficient $q_r^{[1^2 3]}(t, \underline{m}^2)$ are $26 + r$ with $0 \leq r \leq 8$.
 - $m_1 \neq m_2 = m_3 \neq m_4 = m_5$: the degree of the polynomial coefficient $q_r^{[1^2 2]}(t, \underline{m}^2)$ are $33 + r$ with $0 \leq r \leq 8$.
- **The two different mass configuration:** the differential operator has order 6.
 - $m_1 \neq m_2 = m_3 = m_4 = m_5$: the degree of the polynomial coefficient $q_r^{[1^4]}(t, \underline{m}^2)$ are $8 + r$ with $0 \leq r \leq 6$.
 - $m_1 = m_2 \neq m_3 = m_4 = m_5$: the degree of the polynomial coefficient $q_r^{[2 3]}(t, \underline{m}^2)$ are $13 + r$ with $0 \leq r \leq 6$.
- **The all equal mass configuration** $m_1 = m_2 = m_3 = m_4 = m_5$: the differential operator has order 4. The degree of the polynomial coefficient $q_r^{[5]}(t, \underline{m}^2)$ are $1 + r$ with $0 \leq r \leq 4$. This case has been derived in [22, §9].

4.4.1. Mass specialisation. — The Picard–Fuchs operator for the different mass configurations have been derived using the extension of the Griffith–Dwork reduction presented in section 3.3.

We analyse the relation between these different Picard–Fuchs operators. When some masses are identified the order of the Picard–Fuchs operator decreases. By specialising the mass parameters the Picard–Fuchs operator becomes reducible as represented on this diagram



The arrows $P^a \rightarrow P^b$ represent the left factorisation of the differential operator P^a , so that the operator P^b divides the operator P^a as can be checked using the SageMath `ore_algebra` package [65, 66].

The difference here with the three-loop sunset case of section 4.3 is that the order Picard–Fuchs operators decreases by 2 when two masses parameters are identified. It will be explained in [58] that this is a consequence of the changes in the cohomology for Calabi–Yau three-fold geometry determined by the sunset graph polynomial (4.35).

4.5. The five-loop sunset. — In this section we give the result for the Picard–Fuchs operators for the five-loop loop sunset integral

$$\Omega_6^\ominus(t, \underline{m}^2) = \frac{\Omega_0^{(6)}}{\mathcal{F}_6^\ominus(t, \underline{m}^2; \underline{x})} \quad (4.40)$$

with

$$\mathcal{F}_6^\ominus(t, \underline{m}^2; \underline{x}) = tx_1 \cdots x_6 - (m_1^2 x_1 + \cdots + m_6^2 x_6) \left(\frac{1}{x_1} + \cdots + \frac{1}{x_6} \right) x_1 \cdots x_6. \quad (4.41)$$

We list the properties of the Picard–Fuchs operators for all the mass configurations. Numerical results are given on this page [5sunset](#).

- **The six mass configuration** $m_1 \neq m_2 \neq m_3 \neq m_4 \neq m_5 \neq m_6$ **denote** $[1^6]$: the Picard–Fuchs operator of order 29 and degree of the polynomial $q_{29}(t)$ is 521.
- **The five mass configuration** $m_1 \neq m_2 \neq m_3 \neq m_4 \neq m_5 = m_6$ **denoted** $[1^4 2]$: the Picard–Fuchs operator is of order 23 and degree of the polynomial $q_{23}(t)$ is 305.
- **The four mass configuration** $[1^3 3]$ **and** $[1^2 2^2]$: the Picard–Fuchs operator $\mathcal{L}_t^{[1^3 3]}$ is of order 17 and degree of the polynomial $q_{17}^{[1^3 3]}(t)$ is 142, and the Picard–Fuchs operator $\mathcal{L}_t^{[1^2 2^2]}$ is of order 18 and degree of the polynomial $q_{18}^{[1^2 2^2]}(t)$ is 174.
- **The three mass configuration** $[1^2 4]$, $[1 2 3]$ **and** $[2^3]$: the Picard–Fuchs operator $\mathcal{L}_t^{[1^2 4]}$ is of order 12 and degree of the polynomial $q_{12}^{[1^2 4]}(t)$ is 57. The Picard–Fuchs operator $\mathcal{L}_t^{[1 2 3]}$ is of order 13 and degree of the polynomial $q_{13}^{[1 2 3]}(t)$ is 79.
- **The two mass configuration** $[1 5]$, $[2 4]$, $[3^2]$: the Picard–Fuchs operator $\mathcal{L}_t^{[1 5]}$ is of order 8 and degree of the polynomial $q_8^{[1 5]}(t)$ is 20. The Picard–Fuchs operator $L_t^{[2 4]}$ is of order 9 and degree of the polynomial $q_9^{[2 4]}(t)$ is 31. The Picard–Fuchs operator $L_t^{[3^2]}$ is of order 9 and degree of the polynomial $q_9^{[3^2]}(t)$ is 34.
- **The one mass case** $m_1 = \dots = m_6$ $[6]$: the Picard–Fuchs operator is of order 5, the degree of the polynomial $q_5(t)$ is 17. The operator is given in [\[22\]](#).

4.6. The six-loop sunset. — In this section we give the result for the Picard–Fuchs operators for the six-loop loop sunset integral

$$\Omega_7^\ominus(t, \underline{m}^2) = \frac{\Omega_0^{(7)}}{\mathcal{F}_7^\ominus(t, \underline{m}^2; \underline{x})} \quad (4.42)$$

with

$$\mathcal{F}_7^\ominus(t, \underline{m}^2; \underline{x}) = tx_1 \cdots x_7 - (m_1^2 x_1 + \cdots + m_7^2 x_7) \left(\frac{1}{x_1} + \cdots + \frac{1}{x_7} \right) x_1 \cdots x_7. \tag{4.43}$$

In this case the full computation of the Picard–Fuchs operator was not possible. We could only compute it modulo a large prime and the algorithm gave an order of 58 with a degree 2273 for the head polynomial. The order is compatible with the conjecture 4.1.

5. The multi-scoop ice-cream graphs

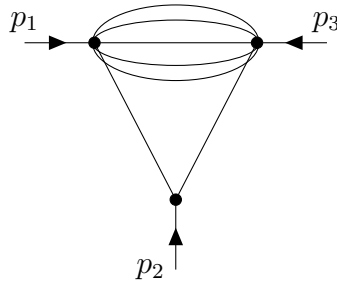


FIGURE 5.1. Multi-loop ice-cream with n loops has $n - 1$ scoops.

The multi-scoop ice-cream graphs represented in fig. 5.1 are three-point graphs, with $p_1 + p_2 + p_3 = 0$, obtained by splitting one edge of the multiloop sunset graphs.

The differential form for the n -scoop ice-cream cone in two dimension in $\mathbb{P}^{n+2}(x_1, \dots, x_{n+3})$ reads

$$\Omega_n(t, \underline{m}^2, \underline{p}^2) = \frac{\mathcal{U}_n(\underline{x})}{\left(\mathcal{U}_n(\underline{x}) \mathcal{L}_n(\underline{m}^2, \underline{x}) - t \mathcal{V}_n(\underline{m}^2, \underline{p}^2; \underline{x}) \right)^2} \Omega_0^{(n+2)} \tag{5.1}$$

with the following graph polynomials

$$\begin{aligned} \mathcal{U}_n(\underline{x}) &:= \left((x_1 + x_2) \left(\sum_{i=3}^{n+3} \frac{1}{x_i} \right) + 1 \right) \prod_{i=3}^{n+3} x_i \\ \mathcal{L}_n(\underline{m}^2, \underline{x}) &= m_1^2 x_1 + \cdots + m_{n+2}^2 x_{n+2} \\ \mathcal{V}_n(\underline{p}^2, \underline{x}) &= \left((p_1^2 x_1 + p_3^2 x_2) + p_2^2 x_1 x_2 \left(\sum_{i=3}^{n+3} \frac{1}{x_i} \right) \right) \prod_{i=3}^{n+3} x_i. \end{aligned} \quad (5.2)$$

The ice-cream graph Jacobian ideal

$$J_n := \left\langle \partial_z \left(\mathcal{U}_n(\underline{x}) \mathcal{L}_n(\underline{m}^2, \underline{x}) - t \mathcal{V}_n(\underline{m}^2, \underline{p}^2; \underline{x}) \right), z \in \{x_1, \dots, x_{n+3}\} \right\rangle \quad (5.3)$$

vanishes for

$$x_{i+3} = x_{j+3} = 0, \quad t p_2^2 x_1 x_2 + (x_1 + x_2) \left(\sum_{\substack{r=0 \\ r \neq i, j}}^n m_{3+r}^2 x_{3+r} \right) = 0, \quad 0 \leq i, j \leq n. \quad (5.4)$$

We will determine the Picard–Fuchs operator with respect to the parameter t

$$\mathcal{L}_t^n = \sum_{r=0}^{o_n} q_r^n(t) \left(\frac{d}{dt} \right)^r \quad (5.5)$$

acting on the multi-scoop ice-cream cone as

$$\mathcal{L}_t^n \left(\frac{\mathcal{U}_n(\underline{x})}{\left(\mathcal{U}_n(\underline{x}) \mathcal{L}_n(\underline{m}^2, \underline{x}) - t \mathcal{V}_n(\underline{m}^2, \underline{p}^2; \underline{x}) \right)^2} \right) = \sum_{i=1}^{n+3} \partial_{x_i} Q_i(\underline{x}, t) \quad (5.6)$$

The certificates Q_i and R_i must not have poles that are not present in the original as discussed in 3.

The results for Picard–Fuchs operator for the zero-scoop ice-cream graph (the triangle graph) in section 5.1, for the one-scoop ice-cream graph in section 5.2 and finally for the two-scoop ice-cream graph in section 5.3.

5.1. The zero-scoop ice-cream (triangle) graph. — In this section we give the Picard–Fuchs operator for the zero-scoop (one-loop)

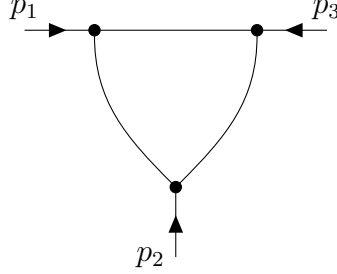


FIGURE 5.2. The zero-scoop (one-loop) ice-cream graph

ice-cream graph of figure 5.2 corresponding to the case $n = 0$ in (5.1) and (5.2). The results are summarised on the page [PF-triangle](#)

With this case we illustrate on this case how the regularity of the certificate affects the form of the differential equation. For the single-scale triangle graph we have for the special configuration $m_1^2 = m_2^2 = m_3^2 = p_2^2 = p_3^2 = 1$ and $p_1^2 = 5$ in the patch $x_3 = 1$

$$\begin{aligned}
& \frac{x_1 + x_2 + 1}{(t(x_1(x_2 - 5) + x_2) - (x_1 + x_2 + 1)^2)^2} \\
&= \partial_{x_1} \left(\frac{(x_2 - 7)(x_1 + x_2 + 1) ((4x_1 + 9)x_2^2 - 5(7x_1 + 6)x_2 + 85x_1 - 15)}{2(t - 9)(x_2 - 5)^2(t(x_1(x_2 - 5) + x_2) - (x_1 + x_2 + 1)^2)^2} \right) \\
& \quad + \partial_{x_1} \left(\frac{-t(x_2 - 7)(x_1^2(x_2 - 5)^2 + x_1((x_2 - 8)x_2 + 35)(x_2 - 5))}{2(t - 9)(x_2 - 5)^2(t(x_1(x_2 - 5) + x_2) - (x_1 + x_2 + 1)^2)^2} \right) \\
& \quad + \partial_{x_1} \left(\frac{-t(x_2 - 7)(x_2((x_2 - 4)x_2 + 10) - 25)}{2(t - 9)(x_2 - 5)^2(t(x_1(x_2 - 5) + x_2) - (x_1 + x_2 + 1)^2)^2} \right) \\
& \quad + \partial_{x_2} \left(\frac{-((x_2 - 7)(t(x_2 - 5)^2 - 4(x_2^2 - 5x_2 - 5))(x_1 + x_2 + 1))}{2(t - 9)(x_2 - 5)(t(x_1(x_2 - 5) + x_2) - (x_1 + x_2 + 1)^2)^2} \right). \tag{5.7}
\end{aligned}$$

The certificat has a pole at $x_2 = 5$ which is not a pole of the original integral. Therefore, integrating over a cycle passing through that pole will not be possible. Since the Feynman integral is defined as integrated over the positive quadrant (2.2), we cannot allow this certificate.

For a regular certificate the Picard–Fuchs operator is order 1 given by

$$\mathcal{L}_t^1 = q_0(t) + q_1(t) \frac{d}{dt} \quad (5.8)$$

with

$$\begin{aligned} q_1(t) = & - \left(tp_2^2 - (m_1 + m_2)^2 \right) \left(tp_2^2 - (m_1 - m_2)^2 \right) \\ & \times \left(m_1^2(p_1^2 - p_2^2 - p_3^2) - m_2^2(p_1^2 + p_2^2 - p_3^2) + 2m_3^2p_2^2 - p_2^2(p_1^2 - p_2^2 + p_3^2)t \right) \\ & \times \left(p_1^2p_2^2p_3^2t^2 + \left(- \left(m_1^2p_3^2(p_1^2 + p_2^2 - p_3^2) \right) + m_2^2p_1^2(p_1^2 - p_2^2 - p_3^2) - m_3^2p_2^2(p_1^2 - p_2^2 + p_3^2) \right) t \right. \\ & \left. + m_1^4p_3^2 - m_1^2 \left(m_2^2(p_1^2 - p_2^2 + p_3^2) + m_3^2(-p_1^2 + p_2^2 + p_3^2) \right) + m_2^4p_1^2 - m_2^2m_3^2(p_1^2 + p_2^2 - p_3^2) + m_3^4p_2^2 \right). \end{aligned} \quad (5.9)$$

The expression for $q_0(t)$ is too large to be displayed here but it is given on this page [PFtriangle](#).

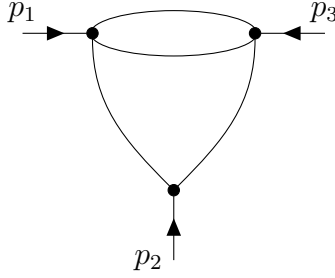


FIGURE 5.3. The one-scoop (two-loop) ice-cream graph

5.2. The one-scoop ice-cream graph. — In this section we give the Picard–Fuchs operator for the one-scoop (two-loop) ice-cream graph of figure 5.3 corresponding to the case $n = 1$ in (5.1) and (5.2).⁽⁶⁾ The results are summarised on the page [PF-icecream-2loop](#).

With a regular certificate the Picard–Fuchs operator is of order 2 and degree 9

$$\mathcal{L}_t^2 = q_0(t) + q_1(t) \frac{d}{dt} + q_2(t) \left(\frac{d}{dt} \right)^2, \quad (5.10)$$

⁽⁶⁾This is sometimes called the Dunce’s cap graph e.g. [67]. But since we are generalising to the multiloop case we will call these graphs ice-cream with multi-scoops.

the higher order coefficient is given by

$$q_2(t) = (tp_2^2 - (m_1 + m_2)^2)(tp_2^2 - (m_1 - m_2)^2)c_1(t)c_2(t)c_3(t) \quad (5.11)$$

with

$$\begin{aligned} c_1(t) = & p_1^2 p_2^2 p_3^2 t^2 + t \left(m_1^2 \left(-p_1^2 p_3^2 - p_2^2 p_3^2 + p_3^4 \right) + m_2^2 \left(p_1^4 - p_1^2 p_2^2 - p_1^2 p_3^2 \right) \right. \\ & \left. + (m_3 + m_4)^2 \left(-p_1^2 p_2^2 + p_2^4 - p_2^2 p_3^2 \right) \right) \\ & + m_1^4 p_3^2 + m_1^2 m_2^2 \left(-p_1^2 + p_2^2 - p_3^2 \right) + m_1^2 (m_3 + m_4)^2 \left(p_1^2 - p_2^2 - p_3^2 \right) \\ & + m_2^4 p_1^2 + m_2^2 (m_3 + m_4)^2 \left(-p_1^2 - p_2^2 + p_3^2 \right) + p_2^2 (m_3 + m_4)^4 \quad (5.12) \end{aligned}$$

and

$$\begin{aligned} c_2(t) = & t^2 p_1^2 p_2^2 p_3^2 + t \left(m_1^2 \left(-p_1^2 p_3^2 - p_2^2 p_3^2 + p_3^4 \right) + m_2^2 \left(p_1^4 - p_1^2 p_2^2 - p_1^2 p_3^2 \right) \right. \\ & \left. + (m_3 - m_4)^2 \left(-p_1^2 p_2^2 + p_2^4 - p_2^2 p_3^2 \right) \right) \\ & + m_1^4 p_3^2 + m_1^2 m_2^2 \left(-p_1^2 + p_2^2 - p_3^2 \right) + m_1^2 (m_3 - m_4)^2 \left(p_1^2 - p_2^2 - p_3^2 \right) + m_2^4 p_1^2 \\ & + m_2^2 (m_3 - m_4)^2 \left(-p_1^2 - p_2^2 + p_3^2 \right) + p_2^2 (m_3 - m_4)^4 \quad (5.13) \end{aligned}$$

and $c_3(t)$ a degree three polynomial which expression is given on the page [PF-icecream-3loop](#). The singularities are located at the roots of $(tp_2^2 - (m_1 + m_2)^2)(tp_2^2 - (m_1 - m_2)^2)c_1(t)c_2(t)$, the roots of $c_3(t)$ are apparent singularities.

The homogeneous differential equation $\mathcal{L}_i^2 f(t) = 0$ is a Liouvillian differential equations that satisfies condition of the theorem 11 of [68]⁽⁷⁾ and the solutions are given by

$$f^\pm(t) = r(t)^{\frac{1}{2}} \exp \left(\pm \int \frac{W(t)}{r(t)} dt \right) \quad (5.14)$$

⁽⁷⁾We thank Charles Doran for this reference.

with

$$r(t) = \frac{r_2(p_2^2)^2 t^2 + r_1 p_2^2 t + r_0}{(tp_2^2 - (m_1 + m_2)^2)(tp_2^2 - (m_1 - m_2)^2)c_1(t)c_2(t)} \quad (5.15)$$

$$W(t) = p_2^2 \frac{c_3(t)^{\frac{5}{2}}}{q_2(t)^{\frac{3}{2}}} \left((p_1^2)^2 + (p_2^2)^2 + (p_3^2)^2 - 2p_1^2 p_2^2 - 2p_1^2 p_3^2 - 2p_2^2 p_3^2 \right) \quad (5.16)$$

and the coefficients

$$\begin{aligned} r_2 &= (p_1^2)^2 + (p_2^2)^2 + (p_3^2)^2 - 2(p_1^2 + p_3^2)p_2^2 \\ r_1 &= \left(-2m_1^2 - 2m_2^2 + 2m_3^2 + 2m_4^2 \right) (p_2^2)^2 \\ &\quad + \left((4m_1^2 + 2m_2^2 - 2m_3^2 - 2m_4^2) p_1^2 + 2p_3^2 (m_1^2 + 2m_2^2 - m_3^2 - m_4^2) \right) p_2^2 \\ &\quad - 2(p_1^2 - p_3^2) (m_1^2 p_1^2 - m_2^2 p_3^2) \\ r_0 &= \left(2m_3^4 + (-2m_1^2 - 2m_2^2 - 4m_4^2) m_3^2 + 2m_4^4 + (-2m_1^2 - 2m_2^2) m_4^2 + m_1^4 + m_2^4 \right) (p_2^2)^2 \\ &\quad - 2(m_1 + m_2)(-m_2 + m_1) (m_1^2 p_1^2 - m_2^2 p_3^2 - (m_3^2 + m_4^2) (p_1^2 - p_3^2)) p_2^2 \\ &\quad + (p_1^2 - p_3^2)^2 (-m_2 + m_1)^2 (m_1 + m_2)^2 \end{aligned}$$

where $W(t)$ is the Wronskian. This indicates that we have a period of a rational surface. This will be proven using a Hodge theoretic analysis for generic physical parameters in [69].

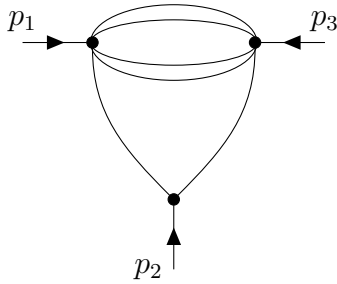


FIGURE 5.4. The two-scoop (three-loop) ice-cream graph

5.3. The two-scoop ice-cream graph. — In this section we give the Picard–Fuchs operator for the two-scoop (three-loop) ice-cream graph in

figure 5.4 corresponding to the case $n = 2$ in (5.1) and (5.2). The results are summarised on the page [PF-icecream-3loop](#).

For this case for any configurations of the internal masses (i.e. with identified masses or all different masses) we find an irreducible Picard–Fuchs equation of order 4. Changing variables from t to $t = 1/z$ the differential operator takes the form

$$\mathcal{L}_z^2 = \sum_{r=0}^4 q_r(z) z^r \left(\frac{d}{dz} \right)^r . \quad (5.17)$$

The operator has for indicial equation $(\rho - 2)^2(\rho - 3)^2 = 0$ near $z = 0$ (or $t = \infty$) which has a two dimension analytic solution near $z = 0$ (or $t = \infty$) with z^r and two non-analytic solutions $z^r \log(z)$ with $r = 2, 3$.⁽⁸⁾

6. Some two-loop graphs differential operator

In this section we give the Picard–Fuchs operator for some two-loop graphs in four dimensions with $D = 4$ in (2.3). The graph differential form of two-loop graph with n internal edges in D dimensions is given by

$$\Omega_n(t) = \frac{(\mathcal{U}_n(\underline{x}))^{n-\frac{3D}{2}}}{(\mathcal{U}_n(\underline{x})\mathcal{L}_n(\underline{m}^2, \underline{x}) - t\mathcal{V}_n(\underline{s}, \underline{x}))^{n-D}} \Omega_0^{(n)} \quad (6.1)$$

with $\mathcal{U}_n(\underline{x})$ homogeneous of degree 2, the kinematic graph polynomial $\mathcal{V}_n(\underline{s}, \underline{x})$ is homogeneous of degree 3, the mass hyperplane $\mathcal{L}_n(\underline{x}) = \sum_{i=1}^n m_i^2 x_i$, and $\Omega_0^{(n)}$ the natural differential form on \mathbb{P}^{n-1} with coordinates $[x_1 : \dots : x_n]$ as defined in (2.4).

The aim of this section is to illustrate the variety of results one can reach using the algorithm presented earlier. We consider the following various cases: the kite graph with $n = 5$ in section 6.1, the Tardigrade

⁽⁸⁾This is a Frobenius basis of solutions that can be obtained from the indicial equation near $t = 0$ [70]. The indicial equation near the point $t = \alpha$ is the equation on the exponents of a solution to the differential equation behaving as $(t - \alpha)^\rho$. In the following we will consider $\alpha = 0$ or $\alpha = \infty$.

with $n = 6$ in section 6.2, the double-box graph with $n = 7$ in section 6.3 and the pentabox graph with $n = 8$ in section 6.4.

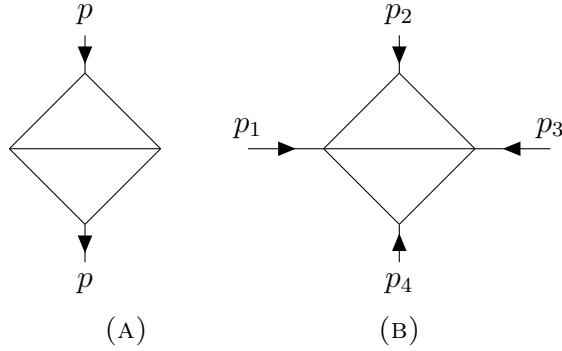


FIGURE 6.1. kite graph

6.1. The kite graph. — In this section we consider the kite integral in fig. 6.1 both in two dimensions and four dimensions.

6.1.1. Triviality of the kite integral in two dimensions. — In two dimensions the rational differential form reads

$$\Omega_{(D=2)\text{kite}}^{n\text{-pt}}(t) = \frac{\mathcal{U}_5(\underline{x})^2}{\mathcal{F}_{\text{kite}}(\underline{m}^2, \underline{s}^2, t; \underline{x})^3} \Omega_0^{(5)} \quad (6.2)$$

with a labelling of the edges where x_5 is associated to the middle line the first Symanzik polynomial reads

$$\mathcal{U}_5(\underline{x}) = (x_1 + x_2)(x_3 + x_4) + (x_1 + x_2 + x_3 + x_4)x_5 \quad (6.3)$$

and the mass hyperplane

$$\mathcal{L}_5(\underline{m}^2, \underline{x}) = m_1^2 x_1 + \cdots + m_5^2 x_5. \quad (6.4)$$

and the graph polynomial

$$\mathcal{F}_{\text{kite}}(\underline{m}^2, \underline{s}^2, t; \underline{x}) = \mathcal{U}_5(\underline{x}) \mathcal{L}_5(\underline{m}^2, \underline{x}) - t \mathcal{V}_{\text{kite}}^{n\text{-pt}}(\underline{s}, \underline{x}). \quad (6.5)$$

For the two points graph in fig. 6.1a the kinematic graph polynomial is given by

$$\mathcal{V}_{\text{kite}}^{2\text{-pt}}(\underline{s}, \underline{x}) = (x_1 + x_4)(x_2 + x_3)x_5 + x_1x_2x_3x_4 \sum_{i=1}^4 \frac{1}{x_i} \quad (6.6)$$

and for the four points graph in fig. 6.1a the kinematic graph polynomial is given by

$$\begin{aligned} \mathcal{V}_{\text{kite}}^{4\text{-pt}}(\underline{s}, \underline{x}) &= (p_1 + p_2)^2 x_2 x_4 x_5 + (p_1 + p_4)^2 x_1 x_3 x_5 \\ &+ p_1^2 x_1 x_4 x_5 + p_2^2 x_1 x_2 (x_3 + x_4 + x_5) + p_3^2 x_2 x_3 x_5 + p_4^2 x_3 x_4 (x_1 + x_2 + x_5), \end{aligned} \quad (6.7)$$

with the momentum conservation condition $p_1 + \dots + p_4 = 0$ and $\{p_1, \dots, p_4\} \in \mathbb{R}^{1,d}$ with $d = 1$ (in two dimensions) or $d = 3$ (in four dimensions).

We first explain that in two dimension the differential for the kite integral is trivial, and give its consequences. A proof of the triviality of the differential form is given afterwards.

In two-dimensions both the two- and four-points cases the integral is trivial because $\mathcal{U}_5(\underline{x})^2$ lies in the Jacobian ideal of $\mathcal{F}_{\text{kite}}(\underline{m}^2, \underline{s}, t; \underline{x})$ because

$$\mathcal{U}_5(\underline{x})^2 = \sum_{i=1}^5 C_i(\underline{x}) \partial_{x_i} \mathcal{F}_{\text{kite}}(\underline{m}^2, \underline{s}^2, t; \underline{x}). \quad (6.8)$$

There is a choice of coefficients $C_i(\underline{x})$ such that

$$\sum_{i=1}^5 \partial_{x_i} C_i(\underline{x}) = 0. \quad (6.9)$$

This implies that

$$\frac{\mathcal{U}_5(\underline{x})^2}{\mathcal{F}_{\text{kite}}(\underline{m}^2, \underline{s}^2, t; \underline{x})^3} = -\frac{1}{2} \sum_{i=1}^5 \partial_{x_i} \frac{C_i(\underline{x})}{\mathcal{F}_{\text{kite}}(\underline{m}^2, \underline{s}^2, t; \underline{x})^2}. \quad (6.10)$$

This implies that the differential form in (6.2) is trivial

$$\Omega_{(D=2)\text{kite}}^{n\text{-pt}}(t) = d\beta_{(D=2)\text{kite}}^{n\text{-pt}}. \quad (6.11)$$

As a consequence the kite integral Feynman in $D = 2$ reduces to its boundary components given by a sum of four one-scoop ice-cream like Feynman integrals (from the boundaries at $x_i = 0$ with $1 \leq i \leq 4$) and a product of two one-loop integral from $x_5 = 0$. There is no contributions from $x_i = \infty$ with $1 \leq i \leq 5$ as can be checked on the expressions given on the page [PF-kite](#).

We give a proof of the reduction in (6.8) with the condition (6.9). The coefficients $C_i(\underline{x})$ are homogeneous polynomial of degree 2 in the variables $\underline{x} = \{x_1, \dots, x_5\}$

$$C_i(\underline{x}) = \sum_{\substack{a_1 + \dots + a_5 = 0 \\ 0 \leq a_i \leq 2}} c_i(a_1, \dots, a_5) \prod_{r=1}^5 x_r^{a_r}. \quad (6.12)$$

Each polynomial has 15 coefficients. The condition (6.9) leads to five linear equations, that we can solve for, say $c_5(0, 0, 0, 0, 2)$, $c_5(0, 0, 0, 1, 1)$, $c_5(0, 0, 1, 0, 1)$, $c_5(0, 1, 0, 0, 1)$, $c_5(1, 0, 0, 0, 1)$. We set to zero the coefficients

$$\begin{aligned} c_2(1, 0, 1, 0, 0) &= c_3(0, 1, 1, 0, 0) = c_3(0, 2, 0, 0, 0) = c_3(1, 0, 0, 1, 0) \\ &= c_3(1, 0, 1, 0, 0) = c_3(1, 1, 0, 0, 0) = c_3(2, 0, 0, 0, 0) = c_4(0, 1, 1, 0, 0) \\ &= c_4(0, 2, 0, 0, 0) = c_4(1, 0, 0, 1, 0) = c_4(1, 0, 1, 0, 0) = c_4(1, 1, 0, 0, 0) \\ &= c_4(2, 0, 0, 0, 0) = c_5(0, 1, 1, 0, 0) = c_5(0, 2, 0, 0, 0) = c_5(1, 0, 0, 1, 0) \\ &= c_5(1, 0, 1, 0, 0) = c_5(1, 1, 0, 0, 0) = c_5(2, 0, 0, 0, 0) = 0. \end{aligned} \quad (6.13)$$

The Jacobian reduction in (6.8) leads to 64 linear equations in the remaining 51 coefficients of the polynomial C_i , denoted \vec{C} ,

$$A\vec{C} = \vec{B} \quad (6.14)$$

with $B^T = \{0, 0, 1, 0, 0, 0, 2, 0, 0, 1, 0, 0, 0, 0, 0, 2, 2, 0, 2, 4, 0, 2, 0, 0, 1, 2, 1, 2, 2, 1, 0, 0, 0, 0, 2, 2, 0, 2, 4, 0, 2, 0, 0, 2, 4, 2, 4, 4, 2, 0, 0, 0, 1, 2, 1, 2, 2, 1, 0, 0, 0, 0, 0\}$. The matrix A has rank 47 for the two-point case, and rank 51 for the four-point case. The system has a unique solution in the

two-point case, but it has a unique solution only when the momenta $\{p_1, \dots, p_4\} \in \mathbb{R}^{1,1}$ are in two dimensions. If the momenta are taken in four dimensions $\{p_1, \dots, p_4\} \in \mathbb{R}^{1,3}$, there is no solution to the system and the integral is not trivial anymore.

6.1.2. The kite integral in four dimensions. — In this section we consider the kite integral in four dimensions $D = 4$. The rational differential form in \mathbb{P}^4 associated to the massive two- and four-point kite graph, in fig. 6.1, in four-dimensions read

$$\Omega_{\text{kite}}^{n\text{-pt}}(t) = \frac{\Omega_0^{(5)}}{\mathcal{U}_5(\underline{x})(\mathcal{U}_5(\underline{x})\mathcal{L}_5(\underline{m}^2, \underline{x}) - t\mathcal{V}_{\text{kite}}^{n\text{-pt}}(\underline{s}, \underline{x}))} \quad (6.15)$$

with the $\mathcal{U}_5(\underline{x})$ given in (6.3) and the mass hyperplane $\mathcal{L}_5(\underline{m}^2, \underline{x})$ given in (6.4).

- We start considering the case of the two-point massive kite graph of figure 6.1a studied in [71] by dispersion relations in $D = 4$ dimensions. In this case the kinematic graph polynomial is given in (6.6). In $D = 4$ the Picard–Fuchs operator is given by

$$\mathcal{L}_{(D=4)\text{kite}}^{2\text{-pt}} = t \frac{d}{dt} + 1. \quad (6.16)$$

The Feynman integral satisfies the inhomogeneous differential equation

$$\mathcal{L}_{\text{kite}}^{2\text{-pt}} \int_{x_i \geq 0} \Omega_{\text{kite}}^{2\text{-pt}}(t) = \sum_{i=1}^4 S_i(t). \quad (6.17)$$

where $S_i(t)$ are two-loop sunset like contribution of section 4.2, see the page [PF-kite](#) for the expression for generic mass configurations. This result generalises the special cases with vanishing internal masses considered in [72, 73, 74, 75, 76, 77] derived using other methods.

- We now turn to the four-point case of fig. 6.1b which has for kinematic graph polynomial is given in (6.7). On the numerical cases studied on [PF-kite](#), the algorithm gives seven order operators that factorise using the factorisation algorithm [23] into the product of four differential

operators

$$\mathcal{L}_{\text{kite}}^{4\text{-pt}} = L^{(1)}L^{(2)}L^{(3)}\left(z\frac{d}{dz} + 1\right) \quad (6.18)$$

where $L^{(r)}$ with $r = 1, 2, 3$ are order 2 operators. Although the factorisation is not unique, we still use the one obtained to determine the type of solutions of the differential operator. All the factors have only Liouvillian solutions, as computed by Maple. This can also be checked using a criterion by Falker in Theorem 11 of [68]. Therefore, the product operator $\mathcal{L}_{\text{kite}}^{4\text{-pt}}$ also have only Liouvillian solutions.⁽⁹⁾ This will be proven using a Hodge theoretic analysis for generic physical parameters in [69].

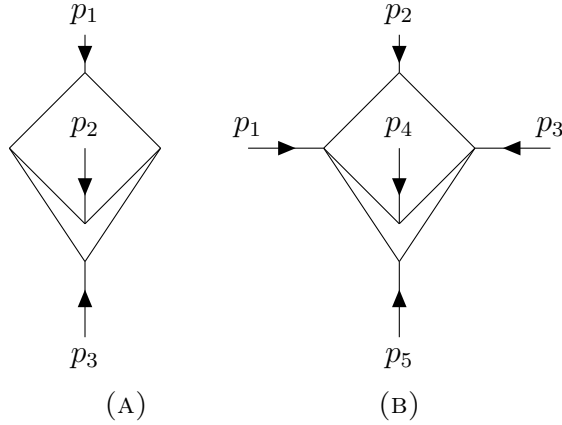


FIGURE 6.2. Tardigrade graph

6.2. The tardigrade. — The tardigrade graphs in fig 6.2 have the rational differential form in \mathbb{P}^5

$$\Omega_{\text{Tardigrade}}^{n\text{-pt}}(t) = \frac{\Omega_0^{(6)}}{\left(\mathcal{U}_6(\underline{x})\mathcal{L}_6(\underline{m}^2, \underline{x}) - t\mathcal{V}_{\text{Tardigrade}}^{n\text{-pt}}(\underline{s}, \underline{x})\right)^2} \quad (6.19)$$

⁽⁹⁾The solutions of a product operator AB are solutions of the inhomogeneous equation $B(y) = u$, where u is a solution of $A(u) = 0$. Using variation of parameters, the solutions of this inhomogeneous equations can be expressed in terms of the solutions of B and that of A , using only the operations defining Liouvillian functions.

with

$$\mathcal{U}_6(\underline{x}) = (x_1 + x_2)(x_3 + x_4) + (x_1 + x_2)(x_5 + x_6) + (x_3 + x_4)(x_5 + x_6) \quad (6.20)$$

the mass hyperplane

$$\mathcal{L}_6(\underline{m}^2, \underline{x}) = m_1^2 x_1 + \cdots + m_6^2 x_6. \quad (6.21)$$

6.2.1. The three points case. — For the three points tardigrade in fig. 6.2a the kinematic graph polynomial is given by

$$\begin{aligned} \mathcal{V}_{\text{Tardigrade}}^{3\text{-pt}}(\underline{s}, \underline{x}) &= p_1^2 (x_1 x_2 (x_3 + x_4 + x_5 + x_6) + x_1 x_4 x_6 + x_2 x_3 x_5) \\ &\quad + p_2^2 x_4 (x_1 (x_3 + x_5) + x_2 (x_3 - x_6) + x_3 (x_5 + x_6)) \\ &\quad + p_3^2 (x_1 x_6 (x_3 + x_5) + x_2 x_6 (x_3 + x_5) + x_2 x_4 (x_5 + x_6) + x_5 x_6 (x_3 + x_4)) \end{aligned} \quad (6.22)$$

with $\{p_1, \dots, p_3\} \in \mathbb{R}^{1,3}$ and $p_1 + p_2 + p_3 = 0$. For generic values of the mass parameters and external momenta the algorithm gives a reducible order 3 Picard–Fuchs operator which is minimal order Picard–Fuchs operator \mathcal{L}_t is of order 2 in t . Near $t = 0$ with one analytic solution behaving as $1/t$ and one logarithmic solution behaving as $\log(t)/t$. Various numerical cases with the analytic solution are given on the page [PF-Tardigrade](#).

In the space case of all equal masses $m_1 = \cdots = m_6$ and all equal kinematics $p_1^2 = p_2^2 = p_3^2$. This is a single scale problem, which can be reabsorbed by redefining $t \rightarrow t m_1^2 / p_1^2$ such that the rational differential form becomes

$$\Omega_{\text{Tardigrade}}^{3\text{-pt}}(t) = \frac{\Omega_0^{(6)}}{m_1^2 \left(\mathcal{U}_6(\underline{x}) \sum_{i=1}^6 x_i - t \mathcal{V}_{\text{Tardigrade}}^{3\text{-pt}}(\underline{x}) \right)^2} \quad (6.23)$$

Then kinematic graph polynomial reads

$$\begin{aligned} \mathcal{V}_{\text{Tardigrade}}^{3\text{-pt}}(\underline{x}) &= x_1 (x_2 x_3 + x_3 (x_4 + x_5 + x_6) + x_4 x_6) + x_1 x_4 (x_2 + x_5) + x_1 x_6 (x_2 + x_5) \\ &\quad + x_2 x_3 (x_4 + x_6 + x_5) + x_5 x_6 (x_2 + x_4) + x_2 x_4 (x_5 + x_6) + x_3 x_5 (x_4 + x_6). \end{aligned} \quad (6.24)$$

In this the minimal order Picard–Fuchs operator is of order 1

$$\mathcal{L}_t = t(t-4)\frac{d}{dt} + 2t - 6. \quad (6.25)$$

6.2.2. The five points case. — For the five points case in fig. 6.2b the kinematic graph polynomial is given by

$$\begin{aligned} \mathcal{V}_{\text{Tardigrade}}^{5\text{-pt}}(\underline{s}, \underline{x}) &= p_1^2 x_1 x_5 (x_3 + x_4) + p_2^2 x_1 x_2 (x_3 + x_4 + x_5 + x_6) + p_3^2 x_2 x_4 (x_5 + x_6) \\ &\quad + p_4^2 x_4 (x_1 (x_3 + x_5) + x_2 (x_3 + x_5) + x_3 (x_5 + x_6)) \\ &\quad + p_5^2 x_5 (x_1 (x_4 + x_6) + x_2 (x_4 + x_6) + x_6 (x_3 + x_4)) \\ &+ (p_1 + p_2)^2 x_2 x_5 (x_3 + x_4) + (p_2 + p_3)^2 x_1 x_4 (x_5 + x_6) + (p_3 + p_4)^2 x_2 (x_3 x_6 - x_4 x_5) \\ &\quad - (p_4 + p_5)^2 x_4 x_5 (x_1 + x_2) + (p_5 + p_1)^2 x_1 (x_3 x_6 - x_4 x_5) \end{aligned} \quad (6.26)$$

with $\{p_1, \dots, p_5\} \in \mathbb{R}^{1,3}$ and $p_1 + \dots + p_5 = 0$. Depending on the configuration of the external momenta the order of the differential operator is between 6 and 11.

- For instance the symmetric case with all equal masses $m_1^2 = \dots = m_6^2$ and $p_1^2 = p_2^2 = p_3^2 = p_4^2 = (p_1 + p_2)^2 = (p_1 + p_4)^2$, by rescaling the t parameter by $t \rightarrow tm_1^2/p_1^2$, the kinematic graph polynomial becomes

$$\begin{aligned} \mathcal{V}_{\text{Tardigrade}}^{5\text{-pt}}(\underline{s}, \underline{x}) &= x_1 (x_2 (x_3 + x_4 + x_5 + x_6) + x_3 (x_4 + x_5 + x_6) + x_5 (x_4 + x_6)) \\ &+ x_2 x_3 (x_4 + x_5) + x_2 x_6 (x_5 - 2x_4) + x_3 x_4 x_5 + x_3 x_4 x_6 + x_3 x_5 x_6 + x_4 x_5 x_6 \end{aligned} \quad (6.27)$$

the algorithm gives a Picard–Fuchs operator is of order 6 that is not factorised by the factorisation algorithm [23] with an head polynomial of degree 50 in t .

- When the masses m_i with $1 \leq i \leq 6$ parameters and the kinematics parameters $p_1^2, p_2^2, p_3^2, p_4^2, (p_1 + p_2)^2, (p_1 + p_4)^2$ take generic values the algorithm gives a Picard–Fuchs operator is of order 11 with an head polynomial of degree up to 215. We have checked using the factorisation algorithm [23] that these differential operators do not

factorise. These results are compatible with the conjecture that the tardigrade Feynman integrals are $K3$ periods integrals [14, 15]. For the case of vanishing masses $m_1 = \dots = m_6 = 0$, the integral will develop new singularities and the order of the Picard–Fuchs operator is expected to decrease.

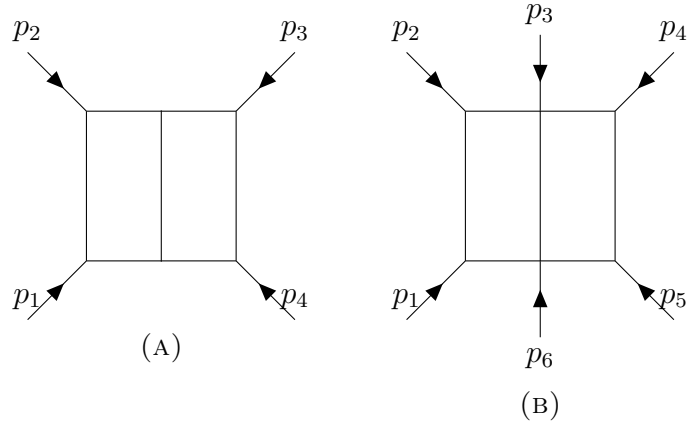


FIGURE 6.3. Double box graphs.

6.3. The double-box graphs. — For the double box graph in fig. 6.3 we have a rational differential form in \mathbb{P}^6

$$\Omega_{\text{Double-box}}^{n\text{-pt}}(t) = \frac{\mathcal{U}_7(\underline{x})}{(\mathcal{U}_7(\underline{x})\mathcal{L}_7(\underline{m}^2, \underline{x}) - t\mathcal{V}_{\text{DoubleBox}}^{n\text{-pt}}(\underline{s}, \underline{x}))^3} \Omega_0^{(7)} \quad (6.28)$$

with a labelling of the edges where the middle internal edge is labelled by the variables x_7 the first Symanzik polynomial reads

$$\mathcal{U}_7(\underline{x}) = (x_1 + x_2 + x_3)(x_4 + x_5 + x_6) + (x_1 + \dots + x_6)x_7 \quad (6.29)$$

the mass hyperplane

$$\mathcal{L}_7(\underline{m}^2, \underline{x}) = m_1^2 x_1 + \dots + m_7^2 x_7 \quad (6.30)$$

- For the four points graph in fig. 6.3a the kinematic graph polynomial reads

$$\begin{aligned}
\mathcal{V}_{\text{DoubleBox}}^{4\text{-pt}}(\underline{s}, \underline{x}) &= p_1^2 x_2 (x_1(x_4+x_5+x_6+x_7)+x_6 x_7) + p_2^2 x_2 (x_3(x_4+x_5+x_6+x_7)+x_4 x_7) \\
&+ p_3^2 x_5 (x_1 x_4 + x_2 x_4 + x_3 x_4 + x_3 x_7 + x_4 x_7) + p_4^2 x_5 (x_1(x_6+x_7) + x_6(x_2+x_3+x_7)) \\
&+ (p_1+p_2)^2 (x_1 x_3 (x_4+x_5+x_6+x_7) + x_1 x_4 (x_6+x_7) + x_6(x_2 x_4 + x_3(x_4+x_7) + x_4 x_7)) \\
&\quad + (p_1+p_4)^2 x_2 x_5 x_7 \quad (6.31)
\end{aligned}$$

with $\{p_1, \dots, p_4\} \in \mathbb{R}^{1,3}$ and $p_1 + \dots + p_4 = 0$.

- For the six points graph in fig. 6.3b the kinematic graph polynomial reads

$$\begin{aligned}
\mathcal{V}_{\text{DoubleBox}}^{6\text{-pt}}(\underline{s}, \underline{x}) &= p_1^2 x_1 x_2 (x_4+x_5+x_6+x_7) + p_2^2 x_2 x_3 (x_4+x_5+x_6+x_7) + p_3^2 x_3 x_6 x_7 \\
&+ p_4^2 x_5 x_6 (x_1+x_2+x_3+x_7) + p_5^2 x_4 x_5 (x_1+x_2+x_3+x_7) + p_6^2 x_1 x_4 x_7 \\
&+ (p_1+p_2)^2 x_1 x_3 (x_4+x_5+x_6+x_7) + (p_1+p_2+p_3)^2 x_1 x_6 x_7 + (p_2+p_3)^2 x_2 x_6 x_7 \\
&\quad + (p_2+p_3+p_4)^2 x_2 x_5 x_7 + (p_3+p_4)^2 x_3 x_5 x_7 + (p_3+p_4+p_5)^2 x_3 x_4 x_7 \\
&+ (p_4+p_5)^2 x_4 x_6 (x_1+x_2+x_3+x_7) + (p_5+p_6)^2 x_1 x_5 x_7 + (p_6+p_1)^2 x_2 x_4 x_7 \quad (6.32)
\end{aligned}$$

with $\{p_1, \dots, p_6\} \in \mathbb{R}^{1,3}$ and $p_1 + \dots + p_6 = 0$. In the six points case we impose the Gram determinant conditions listed in [32] by taking all the kinematics in four dimensions.

We find that both the four- and six-point massive double-box integrals (see figure 6.3a and 6.3b) have a Fuchsian differential operator of order 2 with only regular singularities. We find Picard-Fuchs operators of the form

$$\mathcal{L}_t^{n\text{-pt}} = q_2(t) \left(t \frac{d}{dt} \right)^2 + q_1(t) t \frac{d}{dt} + q_0(t), \quad (6.33)$$

where $q_2(t)$ has single roots different from 0. At $t = 0$ the indicial equation is $(\rho + 1)^2 = 0$ for the six point case, therefore a local basis of solutions behaves as $1/t$ and $\log(t)/t$. Showing that the space of analytic

solutions near $t = 0$ is one dimensional, and there is a logarithmic contribution. This is compatible with the fact that the maximal cut leads to period integral for an elliptic curve [78, 79, 80, 81].

If one does not impose the kinematic conditions implied by the Gram determinant conditions (which means relaxing the condition that the external momenta in a four dimensional space), the Picard–Fuchs operator of order 4. It is not factorisable as certified by the factorisation algorithm [23]. At $t = 0$ the indicial equation is $\rho(\rho - 1)(\rho + 1)^2 = 0$ therefore a local basis of solutions behaves as 1 , t and $1/t$ and $\log(t)/t$. Showing that the space of analytic solutions near $t = 0$ is three-dimensional, and there is a logarithmic contribution. This illustrates how the kinematic relations impose relations between the coefficients of the graph polynomial and affect the singularity structure of the rational differential form. We see that the Gram condition reduces the number of analytic solution near $t = 0$. This will be proven using a Hodge theoretic analysis for generic physical parameters in [69].

These results are given on the page [PF-DoubleBox](#).

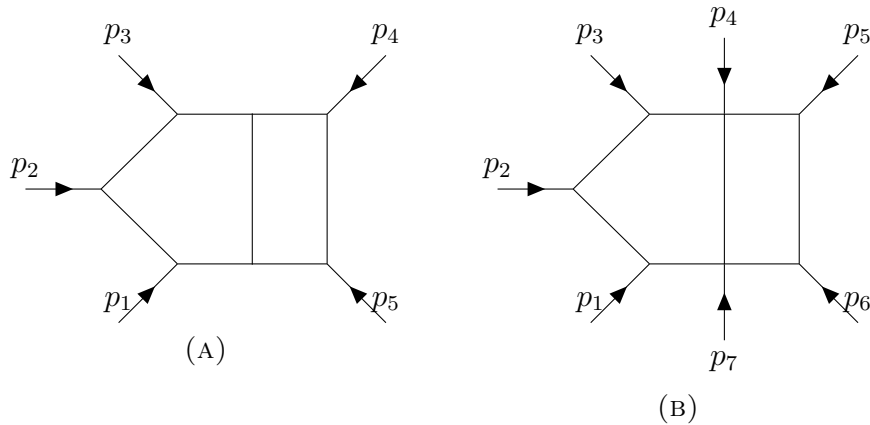


FIGURE 6.4. The Pentabox graphs.

6.4. The pentabox graphs. — For the Pentabox graph in fig. 6.4 we have a rational differential form in \mathbb{P}^7

$$\Omega_{\text{Pentabox}}^{n\text{-pt}}(t) = \frac{\mathcal{U}_8(\underline{x})^2}{\left(\mathcal{U}_8(\underline{x})\mathcal{L}_8(\underline{m}^2, \underline{x}) - t\mathcal{V}_{\text{PentaBox}}^{n\text{-pt}}(\underline{s}, \underline{x})\right)^4} \Omega_0^{(8)} \quad (6.34)$$

with a labelling of the edges where the middle internal edge is labelled by the variables x_8 the first Symanzik polynomial reads

$$\mathcal{U}_8(\underline{x}) = (x_1 + x_2 + x_3 + x_4)(x_5 + x_6 + x_7) + x_8(x_1 + \cdots + x_7) \quad (6.35)$$

the mass hyperplane

$$\mathcal{L}_8(\underline{m}^2, \underline{x}) = m_1^2 x_1 + \cdots + m_8^2 x_8. \quad (6.36)$$

• For the five-point case of figure 6.4a the kinematic graph polynomial is given by

$$\begin{aligned} \mathcal{V}_{\text{Pentabox}}^{5\text{-pt}}(\underline{s}, \underline{x}) &= p_1^2 x_2 (x_1(x_5 + x_6 + x_7 + x_8) + x_5 x_8) + p_2^2 x_2 x_3 (x_5 + x_6 + x_7 + x_8) \\ &+ p_3^2 x_3 (x_4(x_5 + x_6 + x_7 + x_8) + x_7 x_8) + p_4^2 x_6 (x_1 x_7 + x_2 x_7 + x_3 x_7 + x_4 x_7 + x_4 x_8 + x_7 x_8) \\ &+ p_5^2 x_6 (x_1(x_5 + x_8) + x_5(x_2 + x_3 + x_4 + x_8)) + (p_1 + p_2)^2 x_3 (x_1(x_5 + x_6 + x_7 + x_8) + x_5 x_8) \\ &\quad + (p_2 + p_3)^2 x_2 (x_4(x_5 + x_6 + x_7 + x_8) + x_7 x_8) + (p_3 + p_4)^2 x_3 x_6 x_8 \\ &+ (p_4 + p_5)^2 (x_1 x_4 (x_5 + x_6 + x_7 + x_8) + x_1 x_7 (x_5 + x_8) + x_5 (x_2 x_7 + x_3 x_7 + x_4 x_7 + x_4 x_8 + x_7 x_8)) \\ &\quad + (p_5 + p_1)^2 x_2 x_6 x_8, \quad (6.37) \end{aligned}$$

with $\{p_1, \dots, p_5\} \in \mathbb{R}^{1,3}$ and $p_1 + \cdots + p_5 = 0$.

- For the seven-point case of fig. 6.4b the kinematic graph polynomial is given by

$$\begin{aligned}
\mathcal{V}_{\text{PentaBox}}^{7\text{-pt}}(\underline{s}, \underline{x}) &= p_1^2 x_2 (x_1 x_5 + x_1 x_6 + x_1 x_7 + x_1 x_8 + x_5 x_8 + x_6 x_8 + x_7 x_8) \\
&+ p_2^2 x_2 x_3 (x_5 + x_6 + x_7 + x_8) + p_3^2 x_3 (x_4 x_5 + x_4 x_6 + x_4 x_7 + x_4 x_8 + x_7 x_8) \\
&+ p_4^2 x_6 (x_1 x_7 + x_2 x_7 + x_3 x_7 + x_4 x_7 + x_4 x_8 + x_7 x_8) + p_5^2 x_5 x_6 (x_1 + x_2 + x_3 + x_4 + x_8) \\
&\quad + p_6^2 x_5 x_8 (x_1 + x_2 + x_3 + x_4) + p_7^2 x_8 (x_2 + x_3 + x_4) (x_5 + x_6 + x_7) \\
&\quad + (p_1 + p_2)^2 x_3 (x_1 x_5 + x_1 x_6 + x_1 x_7 + x_1 x_8 + x_5 x_8 + x_6 x_8 + x_7 x_8) \\
&+ (p_1 + p_2 + p_3)^2 (x_1 x_4 x_5 + x_1 x_4 x_6 + x_1 x_4 x_7 + x_1 x_4 x_8 - x_2 x_7 x_8 - x_3 x_7 x_8 + x_4 x_5 x_8 + x_4 x_6 x_8) \\
&+ (p_2 + p_3)^2 x_2 (x_4 x_5 + x_4 x_6 + x_4 x_7 + x_4 x_8 + x_7 x_8) + (p_2 + p_3 + p_4)^2 x_2 x_6 x_8 + (p_3 + p_4)^2 x_3 x_6 x_8 \\
&+ (p_3 + p_4 + p_5)^2 x_3 x_5 x_8 + (p_4 + p_5)^2 x_5 (x_1 x_7 + x_2 x_7 + x_3 x_7 + x_4 x_7 + x_4 x_8 + x_7 x_8) \\
&- (p_4 + p_5 + p_6)^2 x_8 (-x_1 x_7 - x_2 x_7 - x_3 x_7 + x_4 x_5 + x_4 x_6) + (p_5 + p_6)^2 x_6 x_8 (x_1 + x_2 + x_3 + x_4) \\
&- (p_5 + p_6 + p_7)^2 x_6 x_8 (x_2 + x_3 + x_4) - (p_6 + p_7)^2 x_5 x_8 (x_2 + x_3 + x_4) + (p_6 + p_7 + p_1)^2 x_2 x_5 x_8 \\
&\quad - (p_7 + p_1)^2 x_2 x_8 (x_5 + x_6 + x_7) - (p_7 + p_1 + p_2)^2 x_3 x_8 (x_5 + x_6 + x_7),
\end{aligned} \tag{6.38}$$

with $\{p_1, \dots, p_7\} \in \mathbb{R}^{1,3}$ and $p_1 + \dots + p_7 = 0$.

For the numerical cases we studied, we find that the five-point massive pentabox integrals in figure 6.4a has a Picard–Fuchs operator of order 2 and degree 18, whereas the seven-point massive pentabox integrals in figure 6.4b has a Picard–Fuchs operator of order 4 and degree 67. We have checked with the factorisation algorithm [23] that these Picard–Fuchs operators are irreducible. We see now a transition in the order of the differential operator when changing the number of external legs.

Near $t = 0$, the indicial equations are $\rho(\rho + 1) = 0$ for the five-point case and $(\rho + 1)\rho(\rho - 1)(\rho - 2) = 0$, for the seven-point case, therefore a canonical local basis of solutions behaves for the five-point case as t^r with $r = -1, 0$, and for the seven-point case as t^r with $r = -1, 0, 1, 2$. We have checked in both case the differential operators have only analytic solution near $t = 0$. In the five-point case for the numerical studied, Maple

identifies the differential equation as being Louvillian. These results are given on the page [PF-Pentabox](#).

This will be proven using a Hodge theoretic analysis for generic physical parameters in [\[69\]](#).

7. Conclusion

In this work we have used the algorithm of [\[26\]](#) for deriving the Picard–Fuchs operator for rational differential form in \mathbb{P}^{n-1}

$$\Omega_n(t) = \frac{\mathcal{U}(\underline{x})^{n-(L+1)D/2}}{(\mathcal{U}(\underline{x})\mathcal{L}_n(\underline{m}^2, \underline{x}) - t\mathcal{V}(\underline{s}, \underline{x}))^{n-LD/2}}\Omega_0^{(n)}, \quad (7.1)$$

with $D = 2$ or $D = 4$. The integration of such differential form over the positive orthant gives the Feynman integrals arising in many physical problems. We have presented the differential operator with respect to the t parameters multiplying the kinematic graph polynomial $\mathcal{V}(\underline{s}, \underline{x})$, but we could have performed the same analysis by considering the differential operator with respect to any of the kinematic coefficient entering the coefficient of the monomials of $\mathcal{V}(\underline{s}, \underline{x})$ or with respect to any of the internal mass \underline{m}^2 in the mass hyperplane $\mathcal{L}(\underline{m}^2, \underline{x})$.

This algorithm is an efficient tool for deriving the homogeneous part of the differential equation satisfied by Feynman integrals, because it spares the computation of the certificates (the Q pieces in [\(1.5\)](#)). It assists the exploration of the changes in the differential operator for various configurations of the physical parameters. These changes reflect a modification in the number of periods integrals implied by modification of the relations between the graph polynomial coefficients.

Our main findings are: (1) to have given some support to the conjecture identifying the multi-loop sunset integrals as relative Calabi–Yau period integrals of dimension $n - 2$. (2) To have given support to the conjecture that the generic tardigrade two-loop integral is a relative period of $K3$

surface of Picard number 11. (3) That the double-box differential operator leads to a second order differential with solutions with logarithmic monodromies, but for the kite and the pentabox graph the differential operator has only Liouvillian solutions. (4) Showed that splitting an edge of the sunset integral to make a multi-scoop ice-cream Feynman integral changes drastically the structure of the differential operator. For instance, at two-loop order the maximal cut of sunset integral is period of an open elliptic curve but the maximal cut of the two-loop ice-cream graph is the one of a rational surface. (5) Exhibiting how various kinematic configurations and the effect of the Gram determinant condition affects the differential operator.

Special values of the kinematics or the mass parameters, changes the structure of the graph polynomials by either providing relation between the monomial or having monomial to vanish. This clearly affects the number of independent period defined by the rational differential form and consequently the order of the Picard–Fuchs operator. The presented algorithm detects these changes. It is tempting to interpret these different values of the physical parameters in the language of the geometric transition.

Acknowledgments

We thank David Broadhurst, Charles Doran, Andrew Harder, Andrey Novoseltsev for discussions and comments. We specially thank Alexandre Goyer and Marc Mezzarobba for help in factoring differential operators. We are grateful to IHES for making their computer resources available. This work has been supported by the ANR grant “Amplitude” ANR-17-CE31-0001-01, the ANR grant “SMAGP” ANR-20-CE40-0026-01, the ANR grant “De Rerum Natura” ANR-19-CE40-0018, and by the European Research Council under the European Union’s Horizon Europe research and innovation programme, grant agreement 101040794 (10000 DIGITS).

References

- [1] V. A. Golubeva, “Some Problems In The Analytic Theory Of Feynman Integrals” , Russ. Math. Surv. **31** 139 (1976)
- [2] F. Pham, “Introduction à l’étude topologique des singularités de Landau”, Paris : Gauthier-Villars; 1967
- [3] E. Panzer, “Feynman Integrals and Hyperlogarithms,” Thesis: PhD Humboldt U. (2015) [[arXiv:1506.07243](#) [math-ph]].
- [4] C. Duhr, “Function Theory for Multiloop Feynman Integrals,” Ann. Rev. Nucl. Part. Sci. **69** (2019), 15-39
- [5] S. Mizera, “Status of Intersection Theory and Feynman Integrals,” PoS **MA2019** (2019), 016 [[arXiv:2002.10476](#) [hep-th]].
- [6] D. J. Broadhurst and D. Kreimer, “Knots and Numbers in Φ^4 Theory to 7 Loops and Beyond,” Int. J. Mod. Phys. C **6** (1995) 519 [[hep-ph/9504352](#)].
- [7] D. J. Broadhurst and D. Kreimer, “Association of Multiple Zeta Values with Positive Knots via Feynman Diagrams Up to 9 Loops,” Phys. Lett. B **393** (1997) 403 [[hep-th/9609128](#)].
- [8] M. Kontsevich and D. Zagier, “Periods”, in Engquist, Björn; Schmid, Wilfried, Mathematics unlimited – 2001 and beyond, Berlin, New York: Springer-Verlag, pp. 771-808.
- [9] S. Bloch, H. Esnault and D. Kreimer, “On Motives associated to graph polynomials,” Commun. Math. Phys. **267** (2006), 181-225 [[arXiv:math/0510011](#) [math.AG]].
- [10] F. C. S. Brown, “On the Periods of Some Feynman Integrals,” [[arXiv:0910.0114](#) [math.AG]].
- [11] S. Bloch, M. Kerr and P. Vanhove, “A Feynman Integral via Higher Normal Functions,” Compos. Math. **151** (2015) no.12, 2329-2375 doi:10.1112/S0010437X15007472 [[arXiv:1406.2664](#) [hep-th]].
- [12] S. Bloch, M. Kerr and P. Vanhove, “Local Mirror Symmetry and the Sunset Feynman Integral,” Adv. Theor. Math. Phys. **21** (2017), 1373-1453 [[arXiv:1601.08181](#) [hep-th]].
- [13] J. L. Bourjaily, Y. H. He, A. J. McLeod, M. Von Hippel and M. Wilhelm, “Traintracks Through Calabi–Yau Manifolds: Scattering Amplitudes Beyond Elliptic Polylogarithms,” Phys. Rev. Lett. **121** (2018) no.7, 071603 [[arXiv:1805.09326](#) [hep-th]].
- [14] J. L. Bourjaily, A. J. McLeod, C. Vergu, M. Volk, M. Von Hippel and M. Wilhelm, “Embedding Feynman Integral (Calabi–Yau) Geometries in Weighted Projective Space,” JHEP **01** (2020), 078 [[arXiv:1910.01534](#) [hep-th]].

- [15] J. L. Bourjaily, A. J. McLeod, M. von Hippel and M. Wilhelm, “Bounded Collection of Feynman Integral Calabi–Yau Geometries,” *Phys. Rev. Lett.* **122** (2019) no.3, 031601 [[arXiv:1810.07689](#) [hep-th]].
- [16] A. Klemm, C. Nega and R. Safari, “The l -loop Banana Amplitude from Gkz Systems and Relative Calabi–Yau Periods,” *JHEP* **04** (2020), 088 [[arXiv:1912.06201](#) [hep-th]].
- [17] K. Bönisch, F. Fischbach, A. Klemm, C. Nega and R. Safari, “Analytic Structure of All Loop Banana Integrals,” *JHEP* **05** (2021), 066 doi:10.1007/JHEP05(2021)066 [[arXiv:2008.10574](#) [hep-th]].
- [18] K. Bönisch, C. Duhr, F. Fischbach, A. Klemm and C. Nega, “Feynman Integrals in Dimensional Regularization and Extensions of Calabi–Yau Motives,” [[arXiv:2108.05310](#) [hep-th]].
- [19] J. L. Bourjaily, J. Broedel, E. Chaubey, C. Duhr, H. Frellesvig, M. Hidding, R. Marzucca, A. J. McLeod, M. Spradlin and L. Tancredi, *et al.* “Functions Beyond Multiple Polylogarithms for Precision Collider Physics,” [[arXiv:2203.07088](#) [hep-ph]].
- [20] A. Forum and M. von Hippel, “A Symbol and Coaction for Higher-Loop Sunrise Integrals,” [[arXiv:2209.03922](#) [hep-th]].
- [21] C. Duhr, A. Klemm, F. Loebbert, C. Nega and F. Porkert, “Yangian-Invariant Fishnet Integrals in 2 Dimensions as Volumes of Calabi–Yau Varieties,” [[arXiv:2209.05291](#) [hep-th]].
- [22] P. Vanhove, “The Physics and the Mixed Hodge Structure of Feynman Integrals,” *Proc. Symp. Pure Math.* **88** (2014), 161-194 [[arXiv:1401.6438](#) [hep-th]].
- [23] F. Chyzak, A. Goyer, and M. Mezzarobba, “Symbolic-Numeric Factorization of Differential Operators”, [[arXiv:2205.08991](#)]
- [24] P. Vanhove “Differential Equations for Feynman Integrals.” Proceedings of the 2021 on International Symposium on Symbolic and Algebraic Computation, 21-26. <https://doi.org/10.1145/3452143.3465512>
- [25] P. Vanhove, “Feynman Integrals, Toric Geometry and Mirror Symmetry,” [[arXiv:1807.11466](#) [hep-th]].
- [26] P. Lairez, “Computing periods of rational integrals”, *Math. Comp.* **85** (2016), 1719-1752, [[arXiv:1404.5069](#)]
- [27] T. Bitoun, C. Bogner, R. P. Klausen and E. Panzer, “Feynman Integral Relations from Parametric Annihilators,” *Lett. Math. Phys.* **109** (2019) no.3, 497-564 [[arXiv:1712.09215](#) [hep-th]].
- [28] Noboru Nakanishi, “Graph Theory and Feynman Integrals”, Gordon & Breach Science Publishers Ltd (1971)
- [29] C. Itzykson and J. B. Zuber, “Quantum Field Theory,” McGraw-Hill, New York, 1980

- [30] C. Bogner and S. Weinzierl, “Feynman Graph Polynomials,” *Int. J. Mod. Phys. A* **25** (2010), 2585-2618 [[arXiv:1002.3458](#) [hep-ph]].
- [31] S. Weinzierl, “Feynman Integrals,” [[arXiv:2201.03593](#) [hep-th]].
- [32] V. E. Asribekov, “Choice of Invariant Variables for the “Many-Point” Functions,” *J. Exp. Theor. Phys.* **15** (1962) no.2, 394
- [33] R. J. Eden, P. V. Landshoff, D. I. Olive and J. C. Polkinghorne, “The analytic S-matrix,” Cambridge University Press, 2002.
- [34] H. S. Hannesdottir and S. Mizera, “What is the $i\epsilon$ for the S-Matrix?,” [[arXiv:2204.02988](#) [hep-th]].
- [35] S. Weinberg, “High-Energy Behavior in Quantum Field Theory,” *Phys. Rev.* **118** (1960), 838-849
- [36] E. R. Speer, “Ultraviolet and Infrared Singularity Structure of Generic Feynman Amplitudes,” *Ann. Inst. H. Poincaré Phys. Theor.* **23** (1975), 1-21
- [37] E. R. Speer, “Generalized Feynman Amplitudes,” vol. 62 of *Annals of Mathematics Studies*. Princeton University Press, New Jersey, Apr., 1969.
- [38] S. Laporta, “Calculation of Master Integrals by Difference Equations,” *Phys. Lett. B* **504** (2001), 188-194 [[arXiv:hep-ph/0102032](#) [hep-ph]].
- [39] A. V. Smirnov and A. V. Petukhov, “The Number of Master Integrals is Finite,” *Lett. Math. Phys.* **97** (2011), 37-44 [[arXiv:1004.4199](#) [hep-th]].
- [40] R. N. Lee and A. A. Pomeransky, “Critical Points and Number of Master Integrals,” *JHEP* **11** (2013), 165 [[arXiv:1308.6676](#) [hep-ph]].
- [41] J. M. Henn, “Lectures on differential equations for Feynman integrals,” *J. Phys. A* **48** (2015), 153001 [[arXiv:1412.2296](#) [hep-ph]].
- [42] I. M. Gelfand, M. M. Kapranov, And A. V. Zelevinsky, “Generalized Euler Integrals and A-Hypergeometric Functions”, *Advances In Mathematics* **84**, 255-271 (1990).
- [43] R. P. Klausen, “Hypergeometric Series Representations of Feynman Integrals by Gkz Hypergeometric Systems,” *JHEP* **04** (2020), 121 [[arXiv:1910.08651](#) [hep-th]].
- [44] T. F. Feng, C. H. Chang, J. B. Chen and H. B. Zhang, “Gkz-Hypergeometric Systems for Feynman Integrals,” *Nucl. Phys. B* **953** (2020), 114952 [[arXiv:1912.01726](#) [hep-th]].
- [45] L. de la Cruz, “Feynman Integrals as A-Hypergeometric Functions,” *JHEP* **12** (2019), 123 [[arXiv:1907.00507](#) [math-ph]].
- [46] O. V. Tarasov, “Connection Between Feynman Integrals Having Different Values of the Space-Time Dimension,” *Phys. Rev. D* **54** (1996) 6479 [[hep-th/9606018](#)].

- [47] C. Koutschan. “HolonomicFunctions (user’s guide).” Technical Report 10-01, RISC Report Series, Johannes Kepler University, Linz, Austria, 2010. <http://www.risc.jku.at/research/combinat/software/HolonomicFunctions/>.
- [48] A. Bostan, P. Lairez, and B. Salvy, “Creative telescoping for rational functions using the Griffiths–Dwork method.” In Proceedings of the 38th international symposium on symbolic and algebraic computation (pp. 93–100).
- [49] É. Picard. “Quelques remarques sur les intégrales doubles de seconde espèce dans la théorie des surfaces algébriques.”, *C. R. Acad. Sci. Paris*, 129:539–540, 1899.
- [50] P. A. Griffiths. On the periods of certain rational integrals. *Ann. of Math.*, **90** (1969), 460–541.
- [51] B. Dwork. On the zeta function of a hypersurface. *Inst. Hautes Études Sci. Publ. Math.* **12** (1962) 5–68.
- [52] B. Dwork. On the zeta function of a hypersurface: II. *Ann. of Math.*, **80** (1964) 227–299.
- [53] H. Verrill, *Root lattices and pencils of varieties*, *J. Math. Kyoto Univ.* 36 (2) (1996), 423–446.
- [54] V. V. Batyrev, I. Ciocan-Fontanine, B. Kim and D. van Straten, “Conifold transitions and mirror symmetry for Calabi–Yau complete intersections in Grassmannians,” *Nucl. Phys. B* **514** (1998), 640–666 [[arXiv:alg-geom/9710022](https://arxiv.org/abs/alg-geom/9710022) [math.AG]].
- [55] K. Hori and C. Vafa, “Mirror symmetry,” [[arXiv:hep-th/0002222](https://arxiv.org/abs/hep-th/0002222) [hep-th]].
- [56] T. Coates, A. Corti, S. Galkin, V. Golyshev, and A. Kasprzyk, (2012). “Mirror symmetry and Fano manifolds.” European Congress of Mathematics (Kraków, 2-7 July, 2012), November 2013, pp. 285–300 [[arXiv:1212.1722](https://arxiv.org/abs/1212.1722)].
- [57] S. Bloch and P. Vanhove, “The Elliptic Dilogarithm for the Sunset Graph,” *J. Number Theor.* **148** (2015), 328–364 [[arXiv:1309.5865](https://arxiv.org/abs/1309.5865) [hep-th]].
- [58] C. Doran, A. Novoseltsev and P. Vanhove, “Mirroring Towers: The Calabi–Yau Geometry of the Multiloop Sunset Feynman Integrals” to appear.
- [59] P. Candelas, X. de la Ossa, P. Kuusela and J. McGovern, “Mirror Symmetry for Five-Parameter Hulek-Verrill Manifolds,” [[arXiv:2111.02440](https://arxiv.org/abs/2111.02440) [hep-th]].
- [60] S. Müller-Stach, S. Weinzierl and R. Zayadeh, “Picard-Fuchs Equations for Feynman Integrals,” *Commun. Math. Phys.* **326** (2014) 237 [[arXiv:1212.4389](https://arxiv.org/abs/1212.4389) [hep-ph]].

- [61] D. Kreimer, “Bananas: multi-edge graphs and their Feynman integrals,” [[arXiv:2202.05490](https://arxiv.org/abs/2202.05490) [hep-th]].
- [62] S. Müller-Stach, S. Weinzierl and R. Zayadeh, “A Second-Order Differential Equation for the Two-Loop Sunrise Graph with Arbitrary Masses,” *Commun. Num. Theor. Phys.* **6** (2012), 203-222 [[arXiv:1112.4360](https://arxiv.org/abs/1112.4360) [hep-ph]].
- [63] P. Vanhove, “Mirroring towers of Feynman integrals: Fibration and degeneration in Feynman integral Calabi–Yau geometries”, (String Math 2019)
- [64] H. Verrill, *Sums of squares of binomial coefficients, with applications to Picard–Fuchs equations*, [[arXiv:math/0407327](https://arxiv.org/abs/math/0407327)]
- [65] M. Kauers, M. Jaroschek, F. Johansson, “Ore Polynomials In Sage”, http://www.risc.jku.at/research/combinat/software/ore_algebra, [[arXiv 1306.4263](https://arxiv.org/abs/1306.4263)]
- [66] M. Mezzarobba, “Rigorous Multiple-Precision Evaluation of D-Finite Functions in SageMath”, 5th International Congress on Mathematical Software (ICMS 2016), Jul 2016, Berlin, Germany, [[arXiv:1607.01967](https://arxiv.org/abs/1607.01967)]
- [67] R. P. Klausen, “Kinematic singularities of Feynman integrals and principal A-determinants,” *JHEP* **02** (2022), 004 [[arXiv:2109.07584](https://arxiv.org/abs/2109.07584) [hep-th]].
- [68] W. Fakler, “On second order homogeneous linear differential equations with Liouvillian solutions”, *Theoretical Computer Science* **187** (1997) 27-48
- [69] C. Doran, A. Harder, and P. Vanhove, “Motivic geometry of two-loop Feynman integrals” to appear.
- [70] D. R. Morrison, “Picard-Fuchs Equations and Mirror Maps for Hypersurfaces,” *AMS/IP Stud. Adv. Math.* **9** (1998) 185 [[hep-th/9111025](https://arxiv.org/abs/hep-th/9111025)].
- [71] D. J. Broadhurst, “The Master Two Loop Diagram With Masses,” *Z. Phys. C* **47** (1990), 115-124
- [72] E. Remiddi and L. Tancredi, “Differential Equations and Dispersion Relations for Feynman Amplitudes. the Two-Loop Massive Sunrise and the kite Integral,” *Nucl. Phys. B* **907** (2016), 400-444 [[arXiv:1602.01481](https://arxiv.org/abs/1602.01481) [hep-ph]].
- [73] L. Adams, C. Bogner, A. Schweitzer and S. Weinzierl, “The kite Integral to All Orders in Terms of Elliptic Polylogarithms,” *J. Math. Phys.* **57** (2016) no.12, 122302 [[arXiv:1607.01571](https://arxiv.org/abs/1607.01571) [hep-ph]].
- [74] C. Bogner, A. Schweitzer and S. Weinzierl, “Analytic Continuation and Numerical Evaluation of the kite Integral and the Equal Mass Sunrise Integral,” *Nucl. Phys. B* **922** (2017), 528-550 [[arXiv:1705.08952](https://arxiv.org/abs/1705.08952) [hep-ph]].
- [75] C. Bogner, A. Schweitzer and S. Weinzierl, “Analytic Continuation of the kite Family,” [[arXiv:1807.02542](https://arxiv.org/abs/1807.02542) [hep-th]].

- [76] J. Broedel, C. Duhr, F. Dulat, B. Penante and L. Tancredi, “Elliptic Feynman Integrals and Pure Functions,” JHEP **01** (2019), 023 doi:10.1007/JHEP01(2019)023 [[arXiv:1809.10698](#) [hep-th]].
- [77] M. A. Bezuglov, A. I. Onishchenko and O. L. Veretin, “Massive kite Diagrams with Elliptics,” Nucl. Phys. B **963** (2021), 115302 [[arXiv:2011.13337](#) [hep-ph]].
- [78] S. Caron-Huot and K. J. Larsen, “Uniqueness of Two-Loop Master Contours,” JHEP **10** (2012), 026 [[arXiv:1205.0801](#) [hep-ph]].
- [79] S. Bloch, “Double Box Motive,” SIGMA **17** (2021), 048 [[arXiv:2105.06132](#) [math.AG]].
- [80] J. L. Bourjaily, A. J. McLeod, M. Spradlin, M. von Hippel and M. Wilhelm, “Elliptic Double-Box Integrals: Massless Scattering Amplitudes Beyond Polylogarithms,” Phys. Rev. Lett. **120** (2018) no.12, 121603 [[arXiv:1712.02785](#) [hep-th]].
- [81] A. C. Pozo and M. von Hippel, “A Three-Parameter Elliptic Double-Box,” [[arXiv:2209.03921](#) [hep-th]].

September 23, 2022

P. LAIREZ, Inria, Uni. Paris-Saclay, Palaiseau, France

P. VANHOVE, Institut de Physique Théorique, Université Paris-Saclay, CEA, CNRS, F-91191 Gif-sur- Yvette Cedex, France